

CAPITAL UNIVERSITY OF SCIENCE AND
TECHNOLOGY, ISLAMABAD



**MHD Nanofluid Flow With
Cattaneo-Christov Double
Diffusion Model and Chemical
Reaction**

by

Tanzeela Sultan

A thesis submitted in partial fulfillment for the
degree of Master of Philosophy

in the

Faculty of Computing

Department of Mathematics

2022

Copyright © 2022 by Tanzeela Sultan

All rights reserved. No part of this thesis may be reproduced, distributed, or transmitted in any form or by any means, including photocopying, recording, or other electronic or mechanical methods, by any information storage and retrieval system without the prior written permission of the author.

*I dedicate my dissertation work to my **family** and dignified **teachers**. A special feeling of gratitude to, **My Father Mr. Sultan Mehmood and My Mother**, who gave me the encouragement I needed throughout my studies.*



CERTIFICATE OF APPROVAL

MHD Nanofluid flow with Cattaneo-Christov Double Diffusion Model and Chemical Reaction

by

Tanzeela Sultan

(MMT193011)

THESIS EXAMINING COMMITTEE

S. No.	Examiner	Name	Organization
(a)	External Examiner	Dr. Farman Ullah Khan	HITEC, Taxila
(b)	Internal Examiner	Dr. Abdul Rehman Kashif	CUST, Islamabad
(c)	Supervisor	Dr. Muhammad Sagheer	CUST, Islamabad

Dr. Muhammad Sagheer

Thesis Supervisor

November, 2022

Dr. Muhammad Sagheer

Head

Dept. of Mathematics

November, 2022

Dr. M. Abdul Qadir

Dean

Faculty of Computing

November, 2022

Author's Declaration

I, **Tanzeela Sultan**, hereby state that my MPhil thesis titled “**MHD Nanofluid flow with Cattaneo-Christov Double Diffusion Model and Chemical Reaction**” is my own work and has not been submitted previously by me for taking any degree from Capital University of Science and Technology, Islamabad or anywhere else in the country/abroad.

At any time if my statement is found to be incorrect even after my graduation, the University has the right to withdraw my MPhil Degree.

(Tanzeela Sultan)

Registration No: MMT193011

Plagiarism Undertaking

I solemnly declare that research work presented in this thesis titled “**MHD Nanofluid flow with Cattaneo-Christov Double Diffusion Model and Chemical Reaction**” is solely my research work with no significant contribution from any other person. Small contribution/help wherever taken has been dully acknowledged and that complete thesis has been written by me.

I understand the zero tolerance policy of the HEC and Capital University of Science and Technology towards plagiarism. Therefore, I as an author of the above titled thesis declare that no portion of my thesis has been plagiarized and any material used as reference is properly referred/cited.

I undertake that if I am found guilty of any formal plagiarism in the above titled thesis even after award of MPhil Degree, the University reserves the right to with-draw/revoke my MPhil degree and that HEC and the University have the right to publish my name on the HEC/University website on which names of students are placed who submitted plagiarized work.

(Tanzeela Sultan)

Registration No: MMT193011

Acknowledgement

I got no words to articulate my cordial sense of gratitude to **Almighty Allah** who is the most merciful and most beneficent to his creation.

I also express my gratitude to the last prophet of **Almighty Allah, Prophet Muhammad (PBUH)** the supreme reformer of the world and knowledge for human being.

I would like to be thankful to all those who provided support and encouraged me during this work.

I would like to be grateful to my thesis supervisor **Dr. Muhammad Sagheer**, the Head of the Department of Mathematics, for guiding and encouraging towards writing this thesis. It would have remained incomplete without his endeavours. Due to his efforts I was able to write and complete this assertion. Also special thanks to **Dr. Durr e Shehwar** for her valuable suggestions and co-operation and all other faculty members.

I would like to pay great tribute to my **parents**, for their prayers, moral support, encouragement and appreciation.

Last but not the least, I want to express my gratitude to my **friends** especially **Amamma Tul Kubra** who helped me throughout in my MPhil degree.

(**Tanzeela Sultan**)

Abstract

This thesis numerically investigates the influence of aligned magnetic field, Cattaneo-Christov double diffusion model and chemical reaction of the flow of an electrically conducting nanofluid past a nonlinear stretching sheet through a porous medium with frictional heating. The partial differential equations governing the flow problems are converted to ordinary differential equations via similarity variables. The reduced equations are then solved numerically with the aid of shooting method. The influence of physical parameters such as aligned angle, magnetic field strength, dimensionless Maxwell parameter, mixed convection variable, nonlinear thermal variable, gravitational acceleration, relaxation time parameter, Prandtl number Pr , porosity parameter.

Contents

Author's Declaration	iv
Plagiarism Undertaking	v
Acknowledgement	vi
Abstract	vii
List of Figures	x
List of Tables	xi
Abbreviations	xii
Symbols	xiii
1 Introduction	1
1.1 Thesis Contributions	4
1.2 Layout of Thesis	4
2 Preliminaries	5
2.1 Some Basic Terminologies	5
2.2 Types of Fluid	7
2.3 Types of Flow	8
2.4 Modes of Heat Transfer	9
2.5 Dimensionless Numbers	10
2.6 Governing Laws	12
2.7 Shooting Method	13
3 A non-Newtonian flow over stratified stretching/shrinking inclined sheet	16
3.1 Introduction	16
3.2 Mathematical Modeling	16
3.3 Solution Methodology	25
3.4 Results and Discussions	28

4 Cattaneo-Christov model for a non-Newtonian flow over stratified stretching/shrinking inclined sheet	40
4.1 Introduction	40
4.2 Mathematical Modeling	41
4.3 Solution Methodology	47
4.4 Results and Discussions	51
5 Conclusion	64
Bibliography	66

List of Figures

3.1	Geometry for the flow under discussion.	17
3.2	Impact of γ on $f'(\xi)$ for $\epsilon = 1$	32
3.3	Impact of γ on $f'(\xi)$ for $\epsilon = -1$	32
3.4	Impact of β on $f'(\xi)$ for $\epsilon = 1$	33
3.5	Impact of β on f' for $\epsilon = -1$	33
3.6	Impact of δ on temperature	34
3.7	Impact of δ on velocity profile	34
3.8	Impact of Fr on velocity profile	35
3.9	Impact of β_t on velocity	35
3.10	Impact of Pr on temperature profile	36
3.11	Impact of λ_1 on temperature	36
3.12	Impact of α on velocity	37
3.13	Impact of S_1 on temperature profile	37
3.14	Impact of c on temperature	38
3.15	Impact of S on temperature	38
3.16	Impact of Pr and S_1 on Nusselt number	39
4.1	Geometry for the flow under discussion.	41
4.2	Impact of γ on the velocity profile.	56
4.3	Impact of β on the velocity profile.	56
4.4	Impact of δ on the velocity profile.	57
4.5	Impact of δ on the temperature profile.	57
4.6	Impact of Fr on the velocity profile.	58
4.7	Impact of B_t on the velocity.	58
4.8	Impact of Pr on the temperature profile.	59
4.9	Impact of λ_1 on the temperature profile.	59
4.10	Impact of α on the velocity profile.	60
4.11	Impact of S_1 on the temperature profile.	60
4.12	Impact of c on the temperature profile.	61
4.13	Impact of λ_2 on the concentration profile.	61
4.14	Impact of Sc on the concentration profile.	62
4.15	Impact of Sr on the concentration profile.	62
4.16	Impact of λ_3 on the concentration profiles.	63

List of Tables

3.1	30
3.2	31
4.1	53
4.2	54
4.3	Results of $(Re_x)^{\frac{1}{2}}Sh_x$ for $S = 2$ and other various parameters	55

Abbreviations

IVPs	Initial value problems
MHD	Magnetohydrodynamics
ODEs	Ordinary differential equations
PDEs	Partial differential equations
RK	Runge-Kutta

Symbols

C_∞	Ambient concentration
μ	Viscosity
ρ	Density
ν	Kinematic viscosity
τ	Stress tensor
k	Thermal conductivity
α	Thermal diffusivity
σ	Electrical conductivity
u	x -component of fluid velocity
v	y -component of fluid velocity
B_0	Magnetic field constant
k_0	Permeability constant
a	Stretching constant
T_w	Temperature of the wall
T_∞	Ambient temperature of the nanofluid
T	Temperature
ρ_f	Density of the fluid
μ_f	Viscosity of the fluid
ν_f	Kinematic viscosity of the base fluid
ρ_{nf}	Density of the nanofluid
μ_{nf}	Viscosity of the nanofluid
q_r	Radiative heat flux
q	Heat generation constant

q_w	Heat flux
q_m	Mass flux
σ^*	Stefan Boltzmann constant
k^*	Absorption coefficient
ψ	Stream function
ξ	Similarity variable
C_f	Skin friction coefficient
Nu	Nusselt number
Nu_x	Local Nusselt number
Sh	Sherwood number
Sh_x	Local Sherwood number
Re	Reynolds number
Re_x	Local Reynolds number
ϕ	Nanoparticle volume fraction
R	Thermal radiation parameter
n	Stretching parameter
M	Magnetic parameter
K	Permeability parameter
Ec	Eckert number
Pr	Prandtl number
Q	Heat generation parameter
γ_1	Relaxation time parameter
Nb	Brownian motion parameter
Nt	Thermophoresis parameter
γ_2	Chemical reaction parameter
Le	Lewis number
ρ_f	Density of the pure fluid
ρ_s	Density of nanoparticle
μ_f	Viscosity of the base fluid
$(\rho C_p)_f$	Heat capacity of base fluid
$(\rho C_p)_s$	Heat capacity of nanoparticle

σ_f	Electrical conductivity of the base fluid
σ_s	Electrical conductivity of the nanoparticle
k_f	Thermal conductivity of the base fluid
k_s	Thermal conductivity of the nanoparticle
f	Dimensionless velocity
θ	Dimensionless temperature
h	Dimensionless concentration
C	Concentration
C_w	Nanoparticles concentration at the stretching surface

Chapter 1

Introduction

The study of properties of fluid on various surfaces and geometries is one of the most important topics of discussion among researchers because it includes many technological as well as industrial aspects like glass fabric generation, elastic sheets assembling, wire drawing etc [1]. Sakiadis was the first one to examine that boundary layer flow by continuous solid panel flowing with constant speed [2]. Non-Newtonian fluid flowing over the stretched surface has become a topic of critical debate for past few decades. Non-Newtonian fluid play a huge role in many engineering and technological applications. The wide range of applications includes liquids film condensation process, aerodynamics, plastic films emission, copper wire thinnings etc [3]. The most common examples of non-Newtonian fluids in food industry are starch suspension, mayonnaise, yogurts, fruit juices and alcoholic beverages. All the characteristics of these fluids, structures cannot be showed by single constitutive equation. These non-Newtonian fluid models are classified as differential, rate and integral types. Rate type fluid include Maxwell model as it shows the fluid relaxation time phenomenon.

Harris and Wilkinson [4] who presented 2D flow of upper convected Maxwell fluid urged the researchers to find new possibilities. Due to stretching sheet for upper convected Maxwell fluid, the transfer of heat and boundary layer flow have been discussed by many scientists. In past few decades, area of work in fluid dynamics has been heat analysis [5-7].

Heat and mass transfer have many industrial applications like meat and poultry in food industry, plastic and pipe industries, generation of glass fiber, steam generators and electronic devices, streamlined expulsion of plastic sheet, glass blowing, cloth industry etc. Developing an analytical solution and examining two-dimensional flow in the steady fluid induced by a stretching sheet was first done by Crane [8]. Lin and Chen [9] explored the heat transfer features over a persistent stretching area between different surface temperatures. The heat and mass transition referred as blowing over the stretching panel was studied by Laha et al. [10]. The spearheading work of Crane was carried ahead by various researchers indicating the significance of heat transfer flow [11–18].

In fluid dynamics, material which contains pores is known as porous medium. The study of porous medium has huge role in manufacturing and agricultural processes like condensers (used as heat exchange), catalytical plants (used to decrease harmful quality of depleting emanations from automobile engines), gas turbines (utilized to cool gas turbine blades), geophysics and geothermal energy system. The porous media are useful particularly in fermentation process, grain storage, contamination of ground water, generation of gasoline, water motion in petroleum sources, beds of fossil fuel, power conserving areas, petroleum reservoirs, ground water frameworks, thermal storage, depleting radioactives waste units and many others. Liquid flow through porous media in the high velocity systems is an area of great challenge for researchers. Non-parcial porous model is better and improved form of old Darcian model that merge concurrent characteristics of inertial tortuosity drag and boundary features. Henry Darcy, a french engineer, while working on fluid flow through the sand beds developed the flow of heterogeneous liquids by a porous medium in 1856. When inertia and boundary characteristic at a high flow rate are taken in account, the classical Darcy law is ineffective. I.Ullah [19] integrated a square velocity element of Darcian speed to predict the extract boundary layer flow and inertia, to evaluate the inertia and boundary features. This characteristic is credible for high Reynolds number. “Forchheimer phrase” was the name given to the factor by Muskat [20]. Forchheimer on a stretching panel was developed by Pal and Mondal [21].

In adequacy of Darcy-Forchheimer hydro magnetic nanofluid flow in the direction of shrinking panel and the presence of thermal stratification, second order velocity slip, Ohmic dissipation and viscous dissemination impact were inspected by Ganesh et al [22]. Thermal radiation in Non-Darcian hydrophobia medium and the hydromagnetic flow of viscous liquid with viscous dissipation were researched by Gireesha et al [23]. Heat transfer model for the magnetohydrodynamics and the streamwise Darcy-Brinkman-Forchheimer liquid flow were discovered by Rashidi et al [24]. Bejan's thermal lines were used by Ahmed [25] to analyse infused non-Darcy hydrophobia medium with natural as well as forced convection in two sided lid driven enclosure. Hayat et al. [26] examined the Darcy-Forchheimer mobility of viscoelastic nanofluids on account of non-linear stretching sheet. The boundary conditions of Neumann for a standard Darcy-Forcheimer framework was recently investigated by Kang et al. [27].

Magnetic characteristics of electrically conductive liquid, known as Magnetohydrodynamics (MHD) have great role in fluid dynamics. Hannes Alfen used the word MHD for the very first time. MHD flow has a huge importance in industry and is being used in several fields like metallurgical procedures and petroleum production. Cooling speed engaged in these processes plays a vital role in properties of the final result and by use of magnetic field and electrically conductive liquid, the required final product features can be regulated.

Other electrically conductive liquids such as arsenic copper alloys, molten metals, enriched uranium, engine oils, biochemical fluids and other grades etc have different features in the nonattendance as well as in magnetic field view [28]. Nanofluid flows with MHD impact and convective circumstances were examined by Hayat et al. [29]. Passing a porous wedge, the elastic and viscous MHD liquid flow in a mixed convection form was inspected by Hsiao [30].

Ramesh et al. [31] inspected the MHD mixed convection flow of viscoelastic fluid past a stretching plate with Ohmic dissipation. In the presence of the uniform magnetic field, the natural heat transfer of nanofluid inside a longitudinal framework was investigated by Ganji and Malvandi. The effect of associated magnetic

fields on a constant two dimensional flux on a vertical stretching layer is examined by Raju et al. [32]. They found that an increase in the aligned angle lower the velocity profile and enhance the temperature of the fluid.

1.1 Thesis Contributions

In this thesis, first of all the work of Bilal and Muzma Nazeer. [33] will be reviewed. Their work has been extended by considering the Chattaneo-Christov double diffusion model, which is not discussed so far. The given PDEs will be converted into a system of ODEs by applying similarity transformations.

Furthermore, to get the numerical results of non-linear ODEs, the shooting method will be applied. The numerical results are computed by using MATLAB. The impact of different parameters on velocity, temperature, concentration profile along with skin friction, Nusselt number and sherwood number will be discussed through graphs and tables.

1.2 Layout of Thesis

A brief overview of the contents of the thesis is provided below.

Chapter 2 includes some basic definitions and terminologies, which are useful to understand the concepts discussed later on.

Chapter 3 provides the reviewed analytical study of numerical analysis for the non-Newtonian flow over a stratified stretching inclined sheet with the aligned magnetic field and nonlinear convection. The numerical results are derived by the shooting method.

Chapter 4 extends the flow model discussed in Chapter 3 by including the impacts of Chattaneo Cristove Double Diffusion Model and Chemical Reaction.

Chapter 5 provides the concluding remarks of the thesis.

References used in the thesis are mentioned in **Bibliography**.

Chapter 2

Preliminaries

This chapter contains some basic definitions and governing laws, which will be helpful in the subsequent chapters.

2.1 Some Basic Terminologies

Definition 2.1.1 (Fluid)

“A fluid is a substance that deforms continuously under the application of a shear (tangential) stress no matter how small the shear stress may be.” [34]

Definition 2.1.2 (Fluid Mechanics)

“Fluid mechanics is that branch of science which deals with the behavior of the fluid (or gases) at rest as well as in motion.” [35]

Definition 2.1.3 (Fluid Dynamics)

“The study of fluid if the pressure forces are also considered for the fluids in motion, that branch of science is called fluid dynamics.” [35]

Definition 2.1.4 (Fluid Statics)

“The study of fluid at rest is called fluid statics.” [35]

Definition 2.1.5 (Viscosity)

“Viscosity is defined as the property of a fluid which offers resistance to the movement of one layer of fluid over another adjacent layer of the fluid. Mathematically,

$$\mu = \frac{\tau}{\frac{\partial u}{\partial y}},$$

where μ is viscosity coefficient, τ is shear stress and $\frac{\partial u}{\partial y}$ represents the velocity gradient.” [35]

Definition 2.1.6 (Kinematic Viscosity)

“It is defined as the ratio between the dynamic viscosity and density of fluid. It is denoted by symbol ν called ‘**nu**’. Mathematically,

$$\nu = \frac{\mu}{\rho}.” [35]$$

Definition 2.1.7 (Thermal Diffusivity)

“The rate at which heat diffuses by conducting through a material depends on the thermal diffusivity and can be defined as,

$$\alpha = \frac{k}{\rho C_p},$$

where α is the thermal diffusivity, k is the thermal conductivity, ρ is the density and C_p is the specific heat at constant pressure.” [36]

Definition 2.1.8 (Thermal Conductivity)

“The Fourier heat conduction law states that the heat flow is proportional to the

temperature gradient. The coefficient of proportionality is a material parameter known as the thermal conductivity which may be a function of a number of variables.” [37]

2.2 Types of Fluid

Definition 2.2.1 (Ideal Fluid)

“A fluid, which is incompressible and has no viscosity, is known as an ideal fluid. Ideal fluid is only an imaginary fluid as all the fluids, which exist, have some viscosity.” [35]

Definition 2.2.2 (Real Fluid)

“A fluid, which possesses viscosity, is known as a real fluid. In actual practice, all the fluids are real fluids.” [35]

Definition 2.2.3 (Newtonian Fluid)

“A real fluid, in which the shear stress is directly proportional to the rate of shear strain (or velocity gradient), is known as a Newtonian fluid.” [35]

Definition 2.2.4 (Non-Newtonian Fluid)

“A real fluid in which the shear stress is not directly proportional to the rate of shear strain (or velocity gradient), is known as a non-Newtonian fluid.

$$\tau_{xy} \propto \left(\frac{du}{dy} \right)^m, \quad m \neq 1$$

$$\tau_{xy} = \mu \left(\frac{du}{dy} \right)^m .” [35]$$

Definition 2.2.5 (Magnetohydrodynamics)

“Magnetohydrodynamics(MHD) is concerned with the mutual interaction of fluid

flow and magnetic fields. The fluids in question must be electrically conducting and non-magnetic, which limits us to liquid metals, hot ionised gases (plasmas) and strong electrolytes.” [38]

2.3 Types of Flow

Definition 2.3.1 (Rotational Flow)

“Rotational flow is that type of flow in which the fluid particles while flowing along stream-lines, also rotate about their own axis.” [35]

Definition 2.3.2 (Irrotational Flow)

“Irrotational flow is that type of flow in which the fluid particles while flowing along stream-lines, do not rotate about their own axis then this type of flow is called irrotational flow.” [35]

Definition 2.3.3 (Compressible Flow)

“Compressible flow is that type of flow in which the density of the fluid changes from point to point or in other words the density (ρ) is not constant for the fluid, Mathematically,

$$\rho \neq k,$$

where k is constant.” [35]

Definition 2.3.4 (Incompressible Flow)

“Incompressible flow is that type of flow in which the density is constant for the fluid. Liquids are generally incompressible while gases are compressible, Mathematically,

$$\rho = k,$$

where k is constant.” [35]

Definition 2.3.5 (Steady Flow)

“If the flow characteristics such as depth of flow, velocity of flow, rate of flow at any point in open channel flow do not change with respect to time, the flow is said to be steady flow. Mathematically,

$$\frac{\partial Q}{\partial t} = 0,$$

where Q is any fluid property.” [35]

Definition 2.3.6 (Unsteady Flow)

“If at any point in open channel flow, the velocity of flow, depth of flow or rate of flow changes with respect to time, the flow is said to be unsteady. Mathematically,

$$\frac{\partial Q}{\partial t} \neq 0,$$

where Q is any fluid property.” [35]

Definition 2.3.7 (Internal Flow)

“Flows completely bounded by a solid surfaces are called internal or duct flows.” [34]

Definition 2.3.8 (External Flow)

“Flows over bodies immersed in an unbounded fluid are said to be an external flow.” [34]

2.4 Modes of Heat Transfer

Definition 2.4.1 (Heat Transfer)

“Heat transfer is a branch of engineering that deals with the transfer of thermal energy from one point to another within a medium or from one medium to another

due to the occurrence of a temperature difference.” [37]

Definition 2.4.2 (Convection)

“Convection heat transfer is usually defined as energy transport effected by the motion of a fluid. The convection heat transfer between two dissimilar media is governed by Newton’s law of cooling.” [37]

Definition 2.4.3 (Conduction)

“The transfer of heat within a medium due to a diffusion process is called conduction.” [37]

Definition 2.4.4 (Thermal Radiation)

“Thermal radiation is defined as radiant (electromagnetic) energy emitted by a medium and is solely to the temperature of the medium.” [37]

2.5 Dimensionless Numbers

Definition 2.5.1 (Eckert Number)

“It is the dimensionless number used in continuum mechanics. It describes the relation between flows and the boundary layer enthalpy difference and it is used for characterized heat dissipation. Mathematically,

$$Ec = \frac{u^2}{C_p \nabla T}$$

where C_p denotes the specific heat.” [34]

Definition 2.5.2 (Prandtl Number)

“It is the ratio between the momentum diffusivity ν and thermal diffusivity α .

Mathematically, it can be defined as

$$Pr = \frac{\nu}{\alpha} = \frac{\frac{\mu}{\rho}}{\frac{k}{C_p \rho}} = \frac{\mu C_p}{k}$$

where μ represents the dynamic viscosity, C_p denotes the specific heat and k stands for thermal conductivity. The relative thickness of thermal and momentum boundary layer is controlled by Prandtl number. For small Pr , heat distributed rapidly corresponds to the momentum.” [34]

Definition 2.5.3 (Skin Friction Coefficient)

“The steady flow of an incompressible gas or liquid in a long pipe of internal D . The mean velocity is denoted by u_w . The skin friction coefficient can be defined as

$$C_f = \frac{2\tau_0}{\rho u_w^2}$$

where τ_0 denotes the wall shear stress and ρ is the density.” [39]

Definition 2.5.4 (Nusselt Number)

“The hot surface is cooled by a cold fluid stream. The heat from the hot surface, which is maintained at a constant temperature, is diffused through a boundary layer and convected away by the cold stream. Mathematically,

$$Nu = \frac{qL}{k}$$

where q stands for the convection heat transfer, L for the characteristic length and k stands for thermal conductivity.” [40]

Definition 2.5.5 (Sherwood Number)

“It is the nondimensional quantity which show the ratio of the mass transport by convection to the transfer of mass by diffusion. Mathematically:

$$Sh = \frac{kL}{D}$$

here L is characteristics length, D is the mass diffusivity and k is the mass transfer” coefficient.” [41]

Definition 2.5.6 (Reynolds Number)

“It is defined as the ratio of inertia force of a flowing fluid and the viscous force of the fluid. Mathematically,

$$Re = \frac{VL}{\nu},$$

where U denotes the free stream velocity, L is the characteristic length and ν stands for kinematic viscosity.” [35]

2.6 Governing Laws

Governing Law 2.6.1 (Continuity Equation)

“The principle of conservation of mass can be stated as the time rate of change of mass in fixed volume is equal to the net rate of flow of mass across the surface. Mathematically, it can be written as

$$\frac{\partial \rho}{\partial t} + \nabla \cdot (\rho \mathbf{u}) = 0.” [37]$$

Governing Law 2.6.2 (Momentum Equation)

“The momentum equation states that the time rate of change of linear momentum of a given set of particles is equal to the vector sum of all the external forces acting on the particles of the set, provided Newton’s Third Law of action and reaction governs the internal forces. Mathematically, it can be written as:

$$\frac{\partial}{\partial t}(\rho \mathbf{u}) + \nabla \cdot [(\rho \mathbf{u}) \mathbf{u}] = \nabla \cdot \mathbf{T} + \rho \mathbf{g}.” [37]$$

Governing Law 2.6.3 (Energy Equation)

“The law of conservation of energy states that the time rate of change of the total energy is equal to the sum of the rate of work done by the applied forces and

change of heat content per unit time.

$$\frac{\partial \rho}{\partial t} + \nabla \cdot \rho \mathbf{u} = -\nabla \cdot \mathbf{q} + Q + \phi,$$

where ϕ is the dissipation function.” [37]

2.7 Shooting Method

To explain the shooting method, consider the following nonlinear boundary value problem.

$$\left. \begin{aligned} f''(x) &= f(x)f'(x) + 4f(x) \\ f(0) &= 0, \quad f(C) = D. \end{aligned} \right\} \quad (2.1)$$

To decrease the order of the above boundary value problem, establish the following notations.

$$f = Z_1 \quad f' = Z_1' = Z_2 \quad f'' = Z_2'. \quad (2.2)$$

As a result, (2.1) is converted into the following system of first order ODEs.

$$Z_1' = Z_2, \quad Z_1(0) = 0, \quad (2.3)$$

$$Z_2' = Z_1 Z_2 + 4Z_1, \quad Z_2(0) = s, \quad (2.4)$$

where s is the missing initial condition which will be guessed.

The above IVP will be numerically solved by the *RK-4* method. The missing condition s is to be chosen such that.

$$Z_1(C, s) = D. \quad (2.5)$$

For convenience, now onward $Z_1(C, s)$ will be denoted by $Z_1(s)$.

Let us further denote $Z_1(s) - D$ by $H(s)$, so that

$$H(s) = 0. \quad (2.6)$$

The above equation can be solved by using Newton's method with the following iterative formula.

$$s^{n+1} = s^n - \frac{H(s^n)}{\frac{\partial H(s^n)}{\partial s}},$$

or

$$s^{n+1} = s^n - \frac{Z_1(s^n) - D}{\frac{\partial Z_1(s^n)}{\partial s}}. \quad (2.7)$$

To find $\frac{\partial Z_1(s^n)}{\partial s}$, introduce the following notations.

$$\frac{\partial Z_1}{\partial s^n} = Z_3, \quad \frac{\partial Z_2}{\partial s^n} = Z_4. \quad (2.8)$$

As a result of these new notations the Newton's iterative scheme, will then get the form.

$$s^{n+1} = s^n - \frac{Z_1(s) - D}{Z_3(s)}. \quad (2.9)$$

Now differentiating the system of two first order ODEs (2.3)-(2.4) with respect to s , we get another system of ODEs, as follows.

$$Z_3' = Z_4, \quad Z_3(0) = 0. \quad (2.10)$$

$$Z_4' = Z_3 Z_2 + Z_1 Z_4 + 4Z_3, \quad Z_4(0) = 1. \quad (2.11)$$

Writing all the four ODEs (2.3), (2.4), (2.10) and (2.11) together, we have the following initial value problem.

$$\begin{aligned} Z_1' &= Z_2, & Z_1(0) &= 0. \\ Z_2' &= Z_1 Z_2 + 4Z_1, & Z_2(0) &= s. \\ Z_3' &= Z_4, & Z_3(0) &= 0. \\ Z_4' &= Z_3 Z_2 + Z_1 Z_4 + 4Z_3, & Z_4(0) &= 1. \end{aligned}$$

The above system together will be solved numerically by Runge-Kutta method of order four.

The stopping criteria for the Newton's technique is set as,

$$| Z_1(s) - D | < \epsilon,$$

where $\epsilon > 0$ is an arbitrarily small positive number.

Chapter 3

A Non-Newtonian Flow Over Stratified Stretching/Shrinking Inclined Sheet

3.1 Introduction

In this chapter, the numerical analysis of upper-convected Maxwell fluid flow over nonlinear shrinking inclined sheet with inclination angle α is discussed. The nonlinear partial differential equations are converted into dimensionless ODEs by utilizing similarity transformation. To solve these ODEs, shooting method is used. The well known software MATLAB is adopted for numerical computations. At the end, tables and graphs are displayed to show the numerical results of ODEs.

3.2 Mathematical Modeling

Consider a non-Newtonian fluid flowing over an inclined shrinking sheet along with inclination α , aligned magnetic field B_0 with an angle γ and velocity $u_w = ax$ has been considered. The temperature on the wall is $T_f = T_0 + a_1x$ and $T_\infty = T_0 + d_1x$ is the temperature far from the wall.

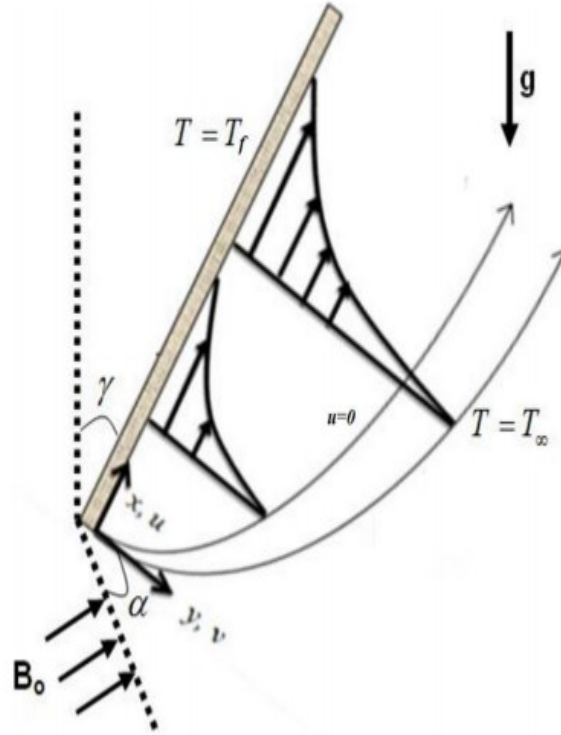


FIGURE 3.1: Geometry for the flow under discussion.

The set of partial differential equations describing the non-Newtonian flow are as follow.

$$\frac{\partial u}{\partial x} + \frac{\partial v}{\partial y} = 0, \quad (3.1)$$

$$\begin{aligned} & u \frac{\partial u}{\partial x} + v \frac{\partial u}{\partial y} + \lambda \left(u^2 \frac{\partial^2 u}{\partial x^2} + v^2 \frac{\partial^2 u}{\partial y^2} + 2uv \frac{\partial^2 u}{\partial x \partial y} \right) \\ &= \nu \frac{\partial^2 u}{\partial y^2} - \frac{\sigma B_0^2}{\rho} \sin^2(\gamma) \left(u + \lambda v \frac{\partial u}{\partial y} \right) + g(\beta_1(T - T_\infty) \\ &+ \beta_2(T - T_\infty)^2) \cos(\alpha) - \frac{v}{k} u - F u^2, \end{aligned} \quad (3.2)$$

$$u \frac{\partial T}{\partial x} + v \frac{\partial T}{\partial y} = \frac{k}{\rho c_p} \frac{\partial^2 T}{\partial y^2}. \quad (3.3)$$

The corresponding BCs have been given as:

$$\left. \begin{aligned} u &= \epsilon u_w(x), \quad v = v_o, \quad T = T_f = T_o + a_1 x, \quad \text{at } y = 0. \\ u &\rightarrow 0, \quad T \rightarrow T_\infty = T_o + d_1 x, \quad \text{as } y \rightarrow \infty. \end{aligned} \right\} \quad (3.4)$$

For the conversion of the mathematical model (3.1)-(3.4) into the system of ODEs, the following similarity transformation has been used.

$$\left. \begin{aligned} \omega(x, y) &= \sqrt{\nu x u_w(x)} f(\xi) = \sqrt{a \nu} x f(\xi), \quad \theta(\xi) = \frac{T - T_\infty}{T_f - T_o}, \\ \xi &= \sqrt{\frac{u_w(x)}{\nu x}} y = \left(\frac{a}{\nu}\right)^{\frac{1}{2}} y. \end{aligned} \right\} \quad (3.5)$$

The detailed procedure for the conversion of (3.1)-(3.3) into the dimensionless form has been discussed below.

$$\begin{aligned} u &= \frac{\partial \omega}{\partial y} \\ \frac{\partial \omega}{\partial y} &= \frac{\partial}{\partial y} (\sqrt{a \nu} x f) \\ &= \sqrt{a \nu} x f' \frac{\partial \xi}{\partial y}. \\ \frac{\partial \xi}{\partial y} &= \sqrt{\frac{a}{\nu}} \\ \frac{\partial \omega}{\partial y} &= a x f' \\ u &= a x f'. \end{aligned} \quad (3.6)$$

$$\begin{aligned} \frac{\partial u}{\partial x} &= \frac{\partial}{\partial x} (a x f') \\ &= a \frac{\partial}{\partial x} (x f'(\xi)) \\ &= a (f' + x f'' \cdot 0) \\ &= a f'. \end{aligned} \quad (3.7)$$

$$\begin{aligned} v &= -\frac{\partial \omega}{\partial x} \\ &= -\frac{\partial}{\partial x} (\sqrt{a \nu} x f) \\ &= -\sqrt{a \nu} \frac{\partial}{\partial x} (x f) \\ &= -\sqrt{a \nu} (f + x f' \cdot 0) \end{aligned}$$

$$v = -\sqrt{a\nu}f \quad (3.8)$$

$$\begin{aligned} \frac{\partial v}{\partial y} &= -\sqrt{a\nu}f' \frac{\partial \xi}{\partial y} \\ &= -\sqrt{a\nu}f' \left(\frac{a}{\nu}\right)^{\frac{1}{2}} \\ &= -af'. \end{aligned} \quad (3.9)$$

Adding (3.7) and (3.9)

$$\frac{\partial u}{\partial x} + \frac{\partial v}{\partial y} = af' - af' = 0. \quad (3.10)$$

Now, the conversion of the momentum equation to get its dimensionless form, will be conducted through the following steps.

$$\begin{aligned} \frac{\partial u}{\partial y} &= \frac{\partial}{\partial y} (axf') \\ &= axf'' \left(\frac{a}{\nu}\right)^{\frac{1}{2}} \\ &= \frac{a^{\frac{3}{2}}x}{\nu^{\frac{1}{2}}} f''. \end{aligned} \quad (3.11)$$

$$\begin{aligned} u \frac{\partial u}{\partial x} &= axf' (af') \\ &= a^2 x f'^2. \end{aligned} \quad (3.12)$$

$$\begin{aligned} v \frac{\partial u}{\partial y} &= -\sqrt{a\nu}f \left(\frac{a^{\frac{3}{2}}x}{\nu^{\frac{1}{2}}} f''\right) \\ &= -a^2 x f f''. \end{aligned} \quad (3.13)$$

$$\begin{aligned} \frac{\partial^2 u}{\partial x^2} &= \frac{\partial}{\partial x} (af') \\ &= af'' \\ &= 0. \end{aligned} \quad (3.14)$$

$$\begin{aligned} \frac{\partial^2 u}{\partial x \partial y} &= af'' \left(\frac{a}{\nu}\right)^{\frac{1}{2}} \\ &= \frac{a^{\frac{3}{2}}}{\nu^{\frac{1}{2}}} f''. \end{aligned} \quad (3.15)$$

$$\frac{\partial^2 u}{\partial y^2} = \frac{a^{\frac{3}{2}}}{\nu^{\frac{1}{2}}} x f''' \left(\frac{a}{\nu}\right)^{\frac{1}{2}}$$

$$= \frac{a^2}{\nu} f''' . \quad (3.16)$$

Putting the above derivatives in the left hand side of (3.2),

$$\begin{aligned} & \frac{\partial u}{\partial x} + v \frac{\partial u}{\partial y} + \lambda \left(u^2 \frac{\partial^2 u}{\partial x^2} + v^2 \frac{\partial^2 u}{\partial y^2} + 2uv \frac{\partial^2 u}{\partial x \partial y} \right) \\ &= a^2 x f'^2 - a^2 x f f'' + \lambda (a^2 x^2 f'^2 . 0 \\ &+ (a\nu f^2) \left(\frac{a^2}{\nu} x f''' \right) + 2(ax f') (-\sqrt{a\nu} f) \left(\frac{a^{\frac{3}{2}}}{\nu^{\frac{1}{2}}} \right) f'' . \end{aligned} \quad (3.17)$$

Now the substitution of derivative in right hand side of (3.2):

$$\begin{aligned} & \nu \frac{\partial^2 u}{\partial y^2} - \frac{\sigma \beta_o^2}{\rho} \sin^2(\gamma) \left(u + \lambda v \frac{\partial u}{\partial y} \right) + g(\beta_1(T - T_\infty) + \beta_2(T - T_\infty)^2) \cos(\alpha) \\ & - \frac{v}{k} u - F u^2 \\ &= \nu \left(\frac{a^2}{\nu} x f''' \right) - \frac{\sigma \beta_o^2}{\rho} \sin^2(\gamma) (ax f') - \lambda (a^2 x f f'') + g(\beta_1(T - T_\infty) \\ &+ \beta_2(T - T_\infty)^2) \cos(\alpha) - \frac{\nu}{k} (ax f') - F (a^2 x^2 f'^2) \\ &= a^2 x f''' - \frac{\sigma B_o^2}{\rho} \sin^2(\gamma) (ax f' - \lambda (a^2 x f f'')) + g(\beta_1(T_f - T_o) \\ &+ \beta_2(T_f - T_o)^2) \cos(\alpha) - \frac{\nu}{ka} x f' - F a^2 x^2 f'^2 \end{aligned} \quad (3.18)$$

Now comparing the right hand side and left hand side of momentum equation (3.2), we get dimensionless form as below .

$$\begin{aligned} & a^2 x (f'^2 - f f'' + \lambda (a f^2 f''') - \lambda (2 a f f' f'')) \\ &= a^2 x (f''' - \frac{\sigma B_o^2}{\rho} \sin^2(\gamma) (f' - \beta f f'')) + g \frac{\beta_1}{a^2 x} (T_f - T_o) (1 + \beta_t \theta) \theta \cos(\alpha) \\ & - \frac{\nu}{ka} f' - F x f'^2) \end{aligned}$$

$$\begin{aligned}
&= f''' + ff'' + \beta(2ff'f'' - f^2f''') + M \sin^2(\gamma)(\beta ff'' - f') \\
&\quad + g \frac{\beta_1}{a^2 x} (T_f - T_o)(1 + \beta_t \theta) \theta \cos(\alpha) - \lambda_1 f' - (1 + Fr)x f'^2 \\
\Rightarrow &f''' + ff'' + \beta(2ff'f'' - f^2f''') + M \sin^2(\gamma)(\beta ff'' - f') \\
&\quad + \delta(1 + \beta_t \theta) \theta \cos(\alpha) - \lambda_1 f' - (1 + Fr)f'^2 = 0.
\end{aligned} \tag{3.19}$$

Next, to find the dimensionless form of temperature equation, the procedure is as follow .

$$\begin{aligned}
\theta(\xi) &= \frac{T - T_\infty}{T_f - T_0} \\
\Rightarrow T &= (T_f - T_0)\theta + T_\infty \\
&= (T_f - T_0)\theta + (T_0 + d_1 x) \\
&= (a_1 x \theta) + (T_0 + d_1 x) \\
\frac{\partial T}{\partial x} &= a_1 \theta + d_1 \\
u \frac{\partial T}{\partial x} &= a x f' (a_1 \theta + d_1) \\
&= a a_1 x \theta f' + a x f' d_1.
\end{aligned} \tag{3.20}$$

$$\begin{aligned}
\frac{\partial T}{\partial y} &= a_1 x \theta' \left(\frac{a}{\nu}\right)^{\frac{1}{2}} \\
v \frac{\partial T}{\partial y} &= -\sqrt{a\nu} f \left(a_1 x \theta' \left(\frac{a}{\nu}\right)^{\frac{1}{2}} \right) \\
&= -a a_1 x f \theta'.
\end{aligned} \tag{3.21}$$

$$\frac{\partial^2 T}{\partial y^2} = a_1 x \theta'' \left(\frac{a}{\nu}\right). \tag{3.22}$$

Using (3.20) and (3.21) for the conversion of left hand side of (3.3),

$$u \frac{\partial T}{\partial x} + v \frac{\partial T}{\partial y} = a a_1 x \theta f' + a x f' d_1 - a a_1 x f \theta'. \tag{3.23}$$

Now using (3.22) in right hand side of (3.3),

we get

$$\begin{aligned}
\frac{\partial^2 T}{\partial y^2} &= \frac{k}{\rho c_p} \left(a_1 x \theta'' \frac{a}{\nu} \right) \\
&= \frac{k}{\rho c_p \nu} a a_1 x \theta'' \\
&= \frac{k}{\rho \nu c_p} a a_1 x \theta'' \\
&= \frac{k}{\mu c_p} a a_1 x \theta'' \\
&= \frac{1}{Pr} a a_1 x \theta''.
\end{aligned} \tag{3.24}$$

Then comparing (3.23) and (3.24) for the dimensionless form of (3.3),

we get

$$\begin{aligned}
a a_1 x \theta f' + a x f' d_1 - a a_1 x f \theta' &= \frac{1}{Pr} a a_1 x \theta''. \\
\Rightarrow a_1 \theta f' + f' - a_1 f \theta' &= \frac{1}{Pr} a_1 \theta''. \\
\Rightarrow \theta f' + \frac{d_1}{a_1} f' - f \theta' &= \frac{1}{Pr} \theta''. \\
\Rightarrow \theta f' + S_1 f' - f \theta' &= \frac{1}{Pr} \theta''. \\
\Rightarrow \frac{1}{Pr} \theta'' + f \theta' - f' \theta - f' S_1 &= 0.
\end{aligned} \tag{3.25}$$

The boundary conditions are converted into dimensionless form through the following steps:

$$\begin{aligned}
\bullet u &= \epsilon u_w & \text{at } y = 0. \\
\Rightarrow a x f'(\xi) &= \epsilon a x & \text{at } \xi = 0. \\
\Rightarrow f'(\xi) &= \epsilon & \text{at } \xi = 0. \\
\Rightarrow f'(0) &= \epsilon & \\
\bullet v &= v_0 & \text{at } y = 0. \\
\Rightarrow -\sqrt{a\nu} f(\xi) &= -\sqrt{a\nu} f(0) & \text{at } \xi = 0. \\
\Rightarrow f(\xi) &= f(0) & .
\end{aligned}$$

$$\begin{aligned}
\bullet T = T_f = T_0 + a_1x & \quad \text{at } y = 0. \\
\Rightarrow \theta(\xi)(T_w - T_\infty) + T_\infty = T_0 + a_1x & \quad \text{at } \xi = 0. \\
\Rightarrow \theta(\xi)(T_0 + a_1x - T_0 - d_1x) + T_0 + d_1x = T_0 + a_1x & \quad \text{at } \xi = 0. \\
\Rightarrow \theta(\xi)(a_1x - d_1x) + d_1x = a_1x & \quad \text{at } \xi = 0. \\
\Rightarrow \theta(0)(a_1 - d_1)x = (a_1 - d_1)x & \quad \text{at } \xi = 0. \\
\Rightarrow \theta(0) = 1 & \\
\bullet u \rightarrow 0 & \quad \text{as } y \rightarrow 0. \\
\Rightarrow axf'(\xi) \rightarrow 0 & \quad \text{as } \xi \rightarrow \infty. \\
\Rightarrow f'(\xi) \rightarrow 0 & \quad \text{as } \xi \rightarrow \infty. \\
\Rightarrow f'(\infty) \rightarrow 0 & \\
\bullet T \rightarrow T_\infty = T_0 + d_1x & \quad \text{as } y \rightarrow \infty. \\
\Rightarrow \theta(\xi)(T_w - T_\infty) + T_\infty \rightarrow T_0 + d_1x & \\
\Rightarrow \theta(\xi)(T_0 + a_1x - T_0 - d_1x) + (T_0 + d_1x) \rightarrow T_0 + d_1x & \\
\Rightarrow \theta(\xi)(a_1x - d_1x) \rightarrow 0 & \\
\Rightarrow \theta(\xi) \rightarrow 0 & \quad \text{as } \xi \rightarrow \infty. \\
\Rightarrow \theta(\infty) \rightarrow 0 & \quad \text{as } \xi \rightarrow \infty.
\end{aligned}$$

The converted BCs are in the following form.

$$\left. \begin{aligned}
f'(0) = \epsilon, \quad f(0) = S, \quad \theta(0) = 1 - S_1 \quad \text{at } \xi = 0, \\
f'(\xi) \rightarrow 0, \quad \theta(\xi) \rightarrow 0, \quad \text{as } \xi \rightarrow \infty.
\end{aligned} \right\} \quad (3.26)$$

The dimensionless forms of (3.2) and (3.3) are:

$$\begin{aligned}
& f''' + f(\xi)f'' + \beta(2ff'f'' - f^2f''') \\
& + M\sin^2(\gamma)(\beta ff'' - f') + \delta(1 + \beta_t\theta)\theta\cos(\alpha) \\
& - \lambda_1 f' - (1 + Fr)f'^2 = 0.
\end{aligned} \quad (3.27)$$

$$\frac{1}{Pr}\theta'' + f\theta' - f'\theta - f'S_1 = 0. \quad (3.28)$$

In (3.27) and (3.28), different parameters are used that are formulated as:

$$\begin{aligned}\delta &= \frac{Gr_x}{Re_x^2}, \quad \beta_t = \frac{\beta_2(T_f - T_0)}{\beta_1}, \quad \lambda_1 = \frac{\nu}{Ka}, \quad Fr = \frac{C_p}{\sqrt{K}}x, \\ Gr_x &= g\beta_1 \frac{(T_f - T_0)x^3}{\nu^2}, \quad Re_x = \frac{xu_w}{\nu}, \quad u_w = ax. \quad Pr = \frac{\mu c_p}{k}, \\ \beta &= \lambda a, \quad M = \sigma \frac{\beta_o^2}{\rho a}, \quad \mu = \rho\nu, \quad S_1 = \frac{d_1}{a_1}.\end{aligned}$$

The skin fraction coefficient is written as:

$$C_f = \frac{(\tau_w)_{y=0}}{\rho u_w^2(x)/2}, \quad (3.29)$$

where

$$\tau_w = \mu \left(\frac{\partial u}{\partial y} \right)_{y=0}.$$

To get non-dimensional form of skin friction the following steps are adopted.

$$\begin{aligned}Cf_x &= \frac{\mu \frac{a^{\frac{3}{2}}}{\nu^{\frac{1}{2}}} x f''(0)}{\rho a^2 x^2 / 2} \\ &= \frac{\mu \sqrt{\frac{ax^2}{\nu}} a f''(0)}{\rho a^2 x^2 / 2} \\ &= \frac{\mu Re_x^{\frac{1}{2}} f''(0)}{\rho \frac{ax^2}{2}} \\ &= \frac{\rho \nu Re_x^{\frac{1}{2}} f''(0)}{\rho u_w x / 2} \\ &= \frac{\nu Re_x^{\frac{1}{2}} f''(0)}{u_w x / 2} \\ &= \frac{Re_x^{\frac{1}{2}} f''(0)}{\frac{Re_x}{2}}. \\ \Rightarrow \frac{1}{2} Re_x^{\frac{1}{2}} Cf_x &= f''(0).\end{aligned} \quad (3.30)$$

Here Reynolds number is given as $Re = \frac{u_w x}{\nu}$.

The local Nusselt number Nu_x is defined as:

$$Nu_x = \frac{xq_w}{k(T_w - T_\infty)}. \quad (3.31)$$

The conversion of the Nusselt number into dimensionless form, has been explained through the following procedure.

$$\begin{aligned} Nu_x &= \frac{xq_w}{k(T_w - T_\infty)} \\ &= \frac{x(-k\frac{\partial T}{\partial y})}{k(T_w - T_\infty)} \\ &= \frac{-x(T_w - T_\infty)\sqrt{\frac{a}{\nu}}\theta'(0)}{(T_w - T_\infty)} \\ &= -\sqrt{\frac{ax^2}{\nu}}\theta'(0) \\ &= -Re_x^{\frac{1}{2}}\theta'(0) \\ \Rightarrow \frac{Nu_x}{Re_x^{\frac{1}{2}}} &= -\theta'(0). \end{aligned} \quad (3.32)$$

3.3 Solution Methodology

In this section, shooting method has been used to obtain the approximate solution of the ordinary differential equation (3.27) and (3.28) along with the boundary conditions. First of all, we need to convert these equations into system of first order ODEs. Let us consider the following notations:

$$\begin{aligned} f &= z_1, & f' &= z'_1 = z_2, & f'' &= z''_1 = z'_2 = z_3, & f''' &= z'_3, \\ \theta &= z_4, & \theta' &= z'_4 = z_5, & \theta'' &= z_5. \end{aligned}$$

Using these notations, the system (3.28) and (3.29) with BCs (3.27) are transformed into the following system of five first order ODEs.

$$\begin{aligned}
 z_1' &= z_2, & z_1(0) &= S, \\
 z_2' &= z_3, & z_2(0) &= c, \\
 z_3' &= (1 - \beta z_1^2)^{-1} (-z_1 z_3 - 2\beta z_1 z_2 z_3 - M \sin^2(\gamma)(\beta z_1 z_3 - z_2) - \delta(1 + \beta_t z_4) z_4 \cos(\alpha) \\
 &\quad + \lambda_1 z_2 + (1 + Fr) z_2^2) & z_3(0) &= p, \\
 z_4' &= z_5, & z_4(0) &= 1 - S_1, \\
 z_5' &= (z_2 z_4 + z_2 S_1 - z_1 z_5) Pr, & z_5(0) &= q,
 \end{aligned}
 \tag{3.33}$$

where p and q are the initial gusses. We take domain $[0, \xi_\infty]$ instead of $[0, \infty)$, where ξ_∞ is a positive real number which is chosen such that there are no noticeable variations in the solution after $\xi = \xi_\infty$. We need to meet the following two conditions.

$$z_2(\xi_\infty, p, q) = 0, \tag{3.34}$$

$$z_4(\xi_\infty, p, q) = 0. \tag{3.35}$$

Newton's method will be used to find p and q . This method has the following iterative scheme.

$$\begin{bmatrix} p \\ q \end{bmatrix}_{n+1} = \begin{bmatrix} p \\ q \end{bmatrix}_n - \begin{bmatrix} \frac{\partial z_2}{\partial p} & \frac{\partial z_2}{\partial q} \\ \frac{\partial z_4}{\partial p} & \frac{\partial z_4}{\partial q} \end{bmatrix}_n^{-1} \begin{bmatrix} z_2 \\ z_4 \end{bmatrix}_n.$$

Now introduce some new notations:

$$\begin{aligned} \frac{\partial z_1}{\partial p} &= z_6, & \frac{\partial z_2}{\partial p} &= z_7, & \frac{\partial z_3}{\partial p} &= z_8, & \frac{\partial z_4}{\partial p} &= z_9, & \frac{\partial z_5}{\partial p} &= z_{10}, \\ \frac{\partial z_1}{\partial q} &= z_{11}, & \frac{\partial z_2}{\partial q} &= z_{12}, & \frac{\partial z_3}{\partial q} &= z_{13}, & \frac{\partial z_4}{\partial q} &= z_{14}, & \frac{\partial z_5}{\partial q} &= z_{15}. \end{aligned}$$

Using the above notations, we get

$$\begin{bmatrix} p \\ q \end{bmatrix}_{n+1} = \begin{bmatrix} p \\ q \end{bmatrix}_n - \begin{bmatrix} z_7 & z_{12} \\ z_9 & z_{14} \end{bmatrix}_n^{-1} \begin{bmatrix} z_2 \\ z_4 \end{bmatrix}_n.$$

The above iterative process will be continued until the following criteria is fulfilled,

$$\max\{|z_2(\xi_\infty, p_n, q_n)|, |z_4(\xi_\infty, p_n, q_n)|\} < \chi, \quad (3.36)$$

where $\chi > 0$ is tolerance which we set as $\chi = 10^{-5}$.

Now to attain another system of ODEs, differentiating the last system of five equations w.r.t p and q , we get

$$\begin{aligned} z'_6 &= z_7, & z_6(0) &= 0, \\ z'_7 &= z_8, & z_7(0) &= 0, \\ z'_8 &= (1 - \beta z_1^2)^{-1} (-z_1 z_8 - z_6 z_3 - 2\beta z_1 z_2 z_8 - 2\beta z_1 z_7 z_3 - 2\beta z_6 z_2 z_3 \\ &\quad - M \sin^2(\gamma)(\beta z_1 z_8 + \beta z_6 z_3 - z_7) - \delta(1 + \beta_t z_9) z_4 \cos(\alpha) - \delta(1 + \beta_t z_4) z_9 \cos(\alpha) \\ &\quad + \lambda_1 z_7 + 2z_2 z_7(1 + Fr)) + (-z_1 z_3 - 2\beta z_1 z_2 z_3 - M \sin^2(\gamma)(\beta z_1 z_3 - z_2) \\ &\quad - \delta(1 + \beta_t z_4) z_4 \cos(\alpha) + \lambda_1 z_2 + (1 + Fr) z_2^2)((1 - \beta z_1^2)^{-2}(2\beta z_1 z_6)), & z_8(0) &= 1, \\ z'_9 &= z_{10}, & z_9(0) &= 0, \\ z_{10} &= Pr(z_7 z_4 + z_2 z_9 + S_1 z_7 - z_6 z_5 - z_1 z_{10}), & z_{10}(0) &= 0, \\ z'_{11} &= z_{12}, & z_{11}(0) &= 0, \\ z'_{12} &= z_{13}, & z_{12}(0) &= 0, \end{aligned}$$

$$\begin{aligned}
z'_{13} = & (1 - \beta z_1^2)^{-1} \left(-z_1 z_{13} - z_{11} z_3 - 2\beta z_1 z_2 z_{13} - 2\beta z_1 z_{12} z_3 - 2\beta z_{11} z_2 z_3 \right. \\
& - M \sin^2(\gamma) (\beta z_1 z_{13} + \beta z_{11} z_3 - z_{12}) - \delta (1 + \beta_t z_{14}) z_4 \cos(\alpha) \\
& - \delta (1 + \beta_t z_4) z_{14} \cos(\alpha) + \lambda_1 z_{12} + 2z_2 z_{12} (1 + Fr) \left. \right) + \left(-z_1 z_3 - 2\beta z_1 z_2 z_3 \right. \\
& - M \sin^2(\gamma) (\beta z_1 z_3 - z_2) - \delta (1 + \beta_t z_4) z_4 \cos(\alpha) + \lambda_1 z_2 + (1 + Fr) z_2^2 \\
& \left. \left((1 - \beta z_1^2)^{-2} (2\beta z_1 z_{11}) \right) \right), \quad z_{13}(0) = 0,
\end{aligned}$$

$$\begin{aligned}
z'_{14} &= z_{15}, & z_{14}(0) &= 0, \\
z_{15} &= Pr(z_{12} z_4 + z_2 z_{14} + S_1 z_{12} - z_{11} z_5 - z_1 z_{15}), & z_{15}(0) &= 1.
\end{aligned}$$

3.4 Results and Discussions

In this section, we analyze the effect of different parameters on the velocity profile and temperature profile by using tables and graphs. In TABLE 3.1 and TABLE 3.2, different parameters are used to calculate numerical values of skin friction $(Re_x)^{\frac{1}{2}} C_f$ and local Nusselt number $(Re_x)^{-\frac{1}{2}} Nu_x$. It is observed that when magnetic parameter M and the injection parameter S are increased, the skin friction and local Nusselt number are increased. By rising, nonlinear thermal variable β_t , Maxwell parameter β , Prandtl number Pr , aligned angle γ , mixed convection variable δ and porosity parameter λ_1 , skin friction $(Re_x)^{\frac{1}{2}} C_f$ and local Nusselt number $(Re_x)^{-\frac{1}{2}} Nu_x$ increase. In these tables, I_f and I_θ are the intervals from which the missing conditions can be chosen.

However, an increase in the thermal stratification variable S_1 and inertia coefficient Fr causes a decrement in the skin friction $(Re_x)^{\frac{1}{2}} C_f$ and local Nusselt number $(Re_x)^{-\frac{1}{2}} Nu_x$. For the decreasing value of the shrinking parameter ϵ , the skin friction increases while the Nusselt number decrease. FIGURE 3.2 shows the behaviour of velocity for various values of γ . By rising the value of γ , the fluid velocity $f'(\xi)$ is devastated. FIGURE 3.3 shows the impact of aligned angle γ on the velocity profile. By increasing the value of γ , the velocity profile escalates.

It can be observed in FIGURE 3.4 that boosting the value of Maxwell parameter β , $f'(\xi)$ is found to demolish. FIGURE 3.5 shows the impact of β on velocity. Increasing the value β causes an increment in $f'(\xi)$. FIGURE 3.6 shows that when mixed convection parameter δ escalates, the temperature profile $\theta(\xi)$ is demolished. It can be observed from FIGURE 3.7 that when δ increases, $f'(\xi)$ increases drastically. FIGURE 3.8 indicates the effect of F_r on velocity. The higher value of F_r reduces the value of $f'(\xi)$.

FIGURE 3.9 shows that when B_t is boosted, the velocity $f'(\xi)$ increased. FIGURE 3.10 indicates the effect of Prandtl number P_r on thermal profile $\theta(\xi)$. When P_r escalates, $\theta(\xi)$ is reduced. FIGURE 3.11 observes that increasing in λ_1 , the temperature profil $\theta(\xi)$ increases. FIGURE 3.12 reveals that when the angle of inclination α is boosted, $f'(\xi)$ decreases. FIGURE 3.13 observes that thermal stratification parameter S_1 is boosted, $\theta(\xi)$ declines. FIGURE 3.14 shows that the impact of shrinking parameter ϵ on the temperature $\theta(\xi)$. When shrinking parameter c is increased, the temperature profile decreases. FIGURE 3.15 indicates that an increment in the injection parameter S causes a decrement in $\theta(\xi)$. FIGURE 3.16 shows the effect of the thermal stratification S_1 and Prandtl number Pr on the Nusselt number. It is observed that the heigher Pr increses the Nusselt number. When S_1 increases, the Nusselt number is decreased.

TABLE 3.1:

Results of $(Re_x)^{\frac{1}{2}}C_f$ for $S = 2$ and other various parameters											
γ	Pr	M	β	Fr	β_t	λ_1	S_1	δ	c	$(Re_x)^{\frac{1}{2}}C_f$	I_f
$\frac{\pi}{6}$	0.7	1	0.1	0.3	0.5	0.3	0.1	0.2	-1	2.728905	[2.1,3.34]
$\frac{\pi}{4}$										2.951310	[2.4,3.42]
$\frac{\pi}{3}$										3.155816	[2.7,3.53]
$\frac{\pi}{2}$										3.347068	[2.9,3.64]
	0.5									2.819168	[2.3,3.43]
	0.9									2.663871	[2.0,3.28]
	1.1									2.616171	[2.0,3.27]
		0								2.480468	[2.0,3.27]
		2								2.951310	[2.4,3.42]
		3								3.155816	[2.7,3.53]
			0							1.898974	[1.0,8.08]
			0.05							2.209428	[1.6,3.04]
			0.15							3.771375	[3.1,4.26]
				0						2.821788	[2.1,3.44]
				0.6						2.631038	[2.1,3.23]
				0.9						2.527297	[2.0,3.12]
					0					2.662509	[2.1,3.21]
					1.0					2.793957	[2.2,3.41]
					1.5					2.857773	[2.2,3.47]
						0.1				2.603259	[1.9,3.37]
						0.5				2.844406	[2.3,3.33]
						0.7				2.951852	[2.5,3.33]
							0.3			2.648688	[1.9,3.29]
							0.5			2.573386	[1.7,3.25]
							0.7			2.503105	[1.5,3.16]
								0		2.370199	[1.7,3.0]
								0.4		3.040205	[2.6,3.68]
								0.6		3.322332	[2.9,3.73]
									-0.4	1.530050	[1.0,2.01]
									-0.6	2.041396	[1.5,2.57]
									-0.8	2.445679	[1.9,3.09]

TABLE 3.2:

Results of $(Re_x)^{-\frac{1}{2}} Nx_u$ for $S = 2$ and other various parameters

γ	Pr	M	β	Fr	β_t	λ_1	S_1	δ	c	$(Re_x)^{-\frac{1}{2}} Nx_u$	I_θ
$\frac{\pi}{6}$	0.7	1	0.1	0.3	0.5	0.3	0.1	0.2	-1	0.926772	[-1.71,-0.4]
$\frac{\pi}{4}$										0.945807	[-1.93,-0.5]
$\frac{\pi}{3}$										0.961403	[-2.04,-0.6]
$\frac{\pi}{2}$										0.974594	[-2.2,-0.8]
	0.5									0.671698	[-0.60,-0.3]
	0.9									1.200992	[-2.09,-0.7]
	1.1									1.489144	[-2.48,-0.9]
		0								0.902379	[-1.60,-0.4]
		2								0.945807	[-1.09,-0.5]
		3								0.961403	[-2.03,-0.6]
			0							0.805105	[-1.84,-0.02]
			0.05							0.860453	[1.82,-0.4]
			0.15							1.009624	[-1.72,-0.4]
				0						0.932396	[-1.93,-0.5]
				0.6						0.920609	[-1.64,-0.3]
				0.9						0.913791	[-1.55,-0.3]
					0					0.919236	[-1.89,-0.3]
					1.0					0.933991	[-1.65,-0.2]
					1.5					0.940923	[-1.74,-0.6]
						0.1				0.915208	[-2.81,-0.5]
						0.5				0.936715	[-1.86,-0.5]
						0.7				0.945428	[-1.96,-0.6]
							0.3			0.655559	[-1.41,-0.2]
							0.5			0.383464	[-100,-0.85]
							0.7			0.110480	[-1.00,-1.84]
								0		0.869786	[-100,-1.85]
								0.4		0.969597	[-2.01,-0.6]
								0.6		1.004387	[-2.0,-0.5]
									-0.4	1.530050	[-2.0,-0.7]
									-0.6	1.099834	[-1.8,-0.5]
									-0.8	1.021087	[-1.8,-0.5]

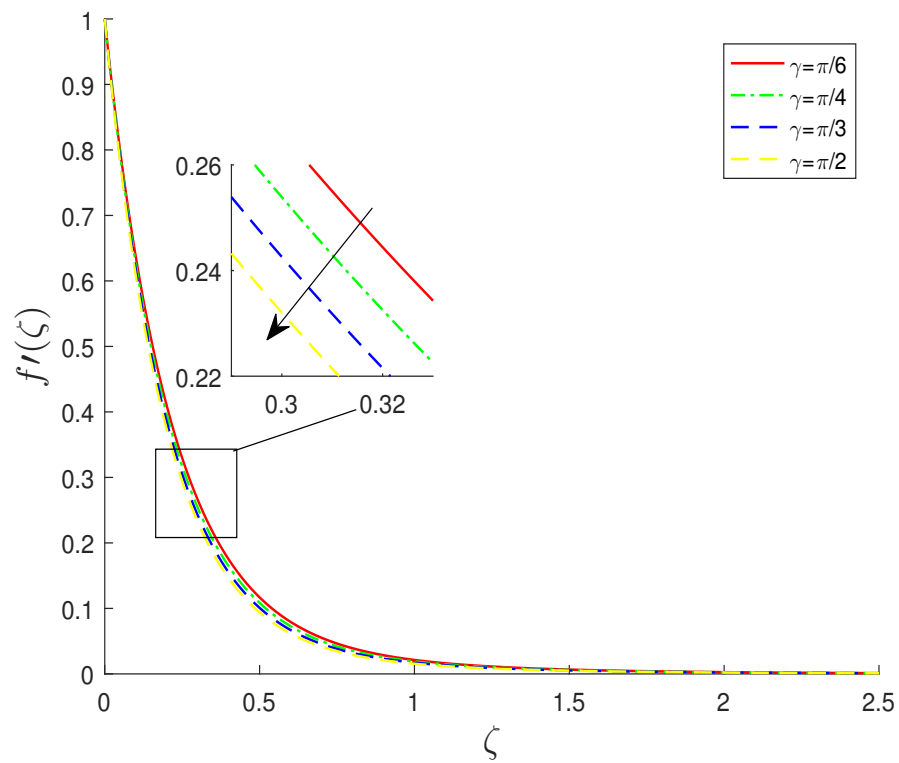


FIGURE 3.2: Impact of γ on $f'(\xi)$ for $\epsilon = 1$.

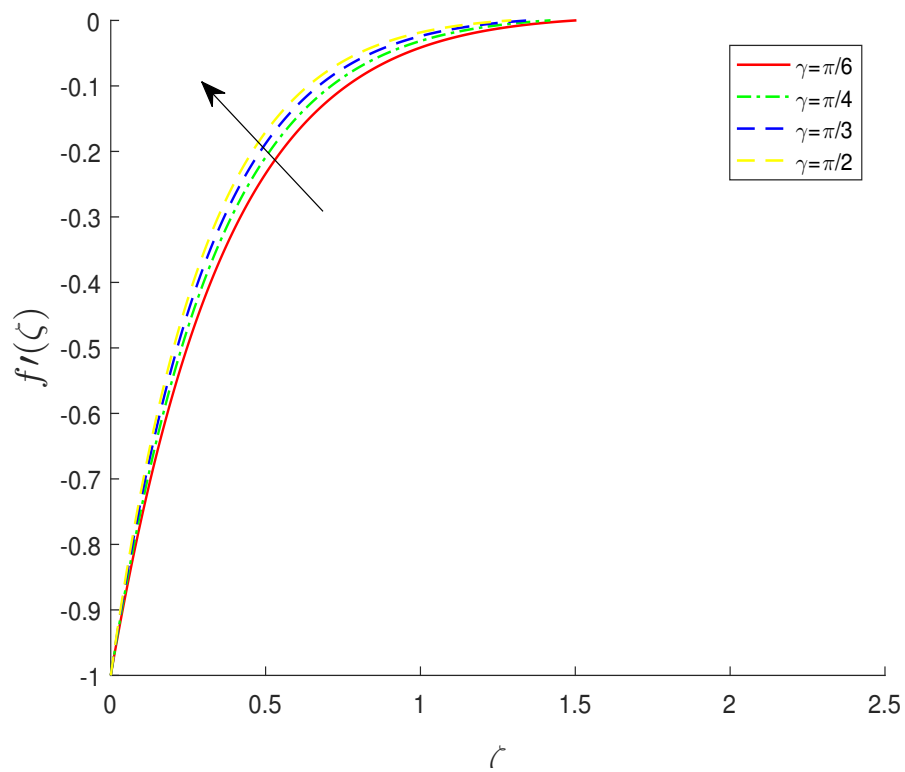


FIGURE 3.3: Impact of γ on $f'(\xi)$ for $\epsilon = -1$.

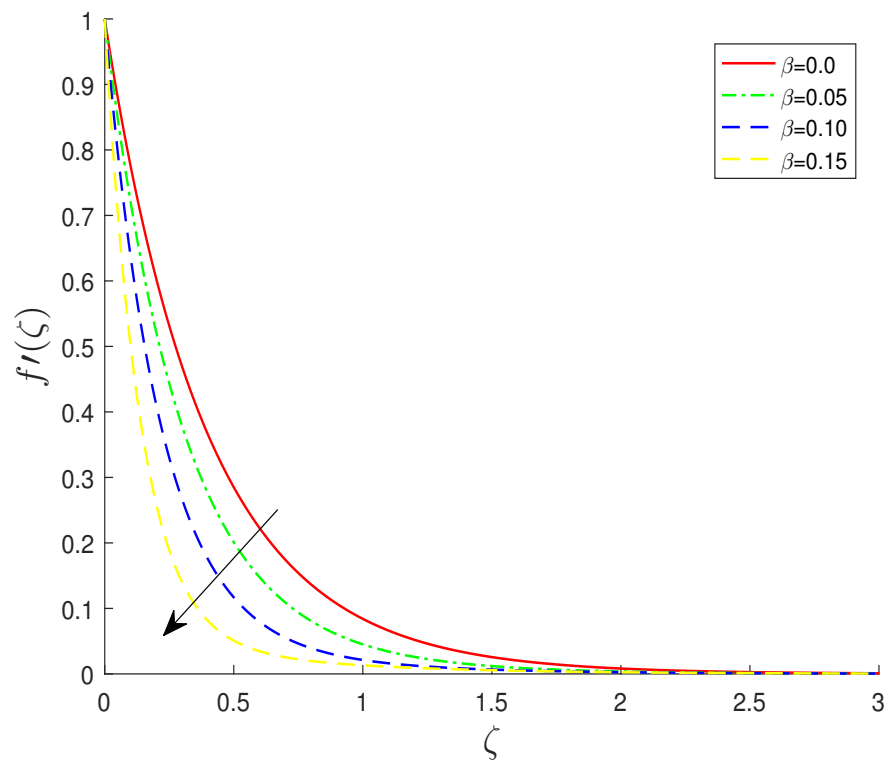


FIGURE 3.4: Impact of β on $f'(\xi)$ for $\epsilon = 1$.

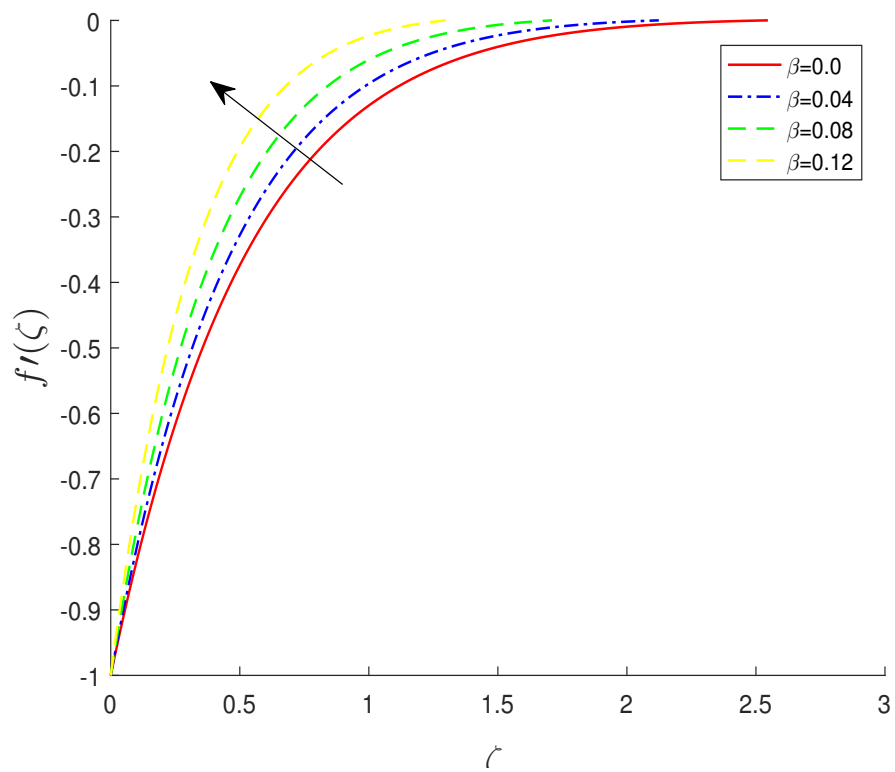


FIGURE 3.5: Impact of β on f' for $\epsilon = -1$.

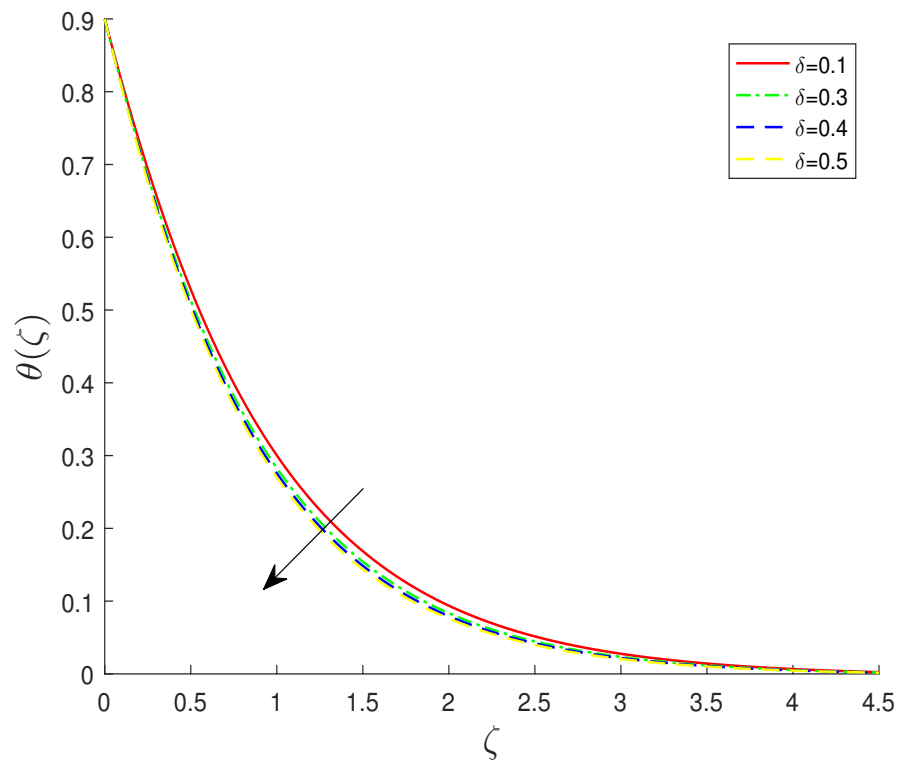


FIGURE 3.6: Impact of δ on temperature

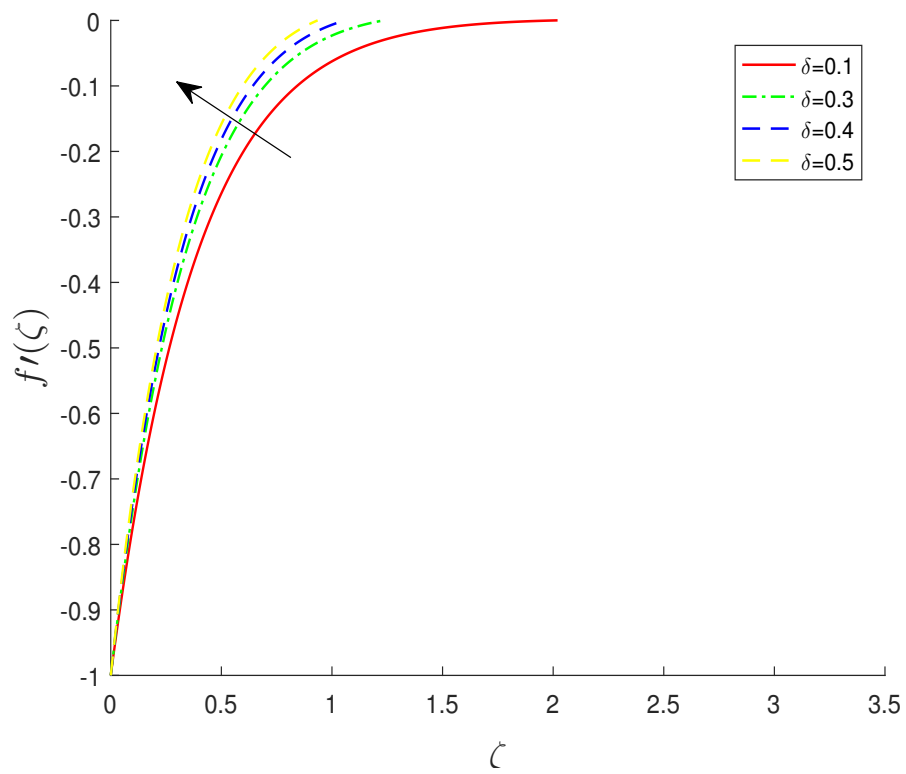


FIGURE 3.7: Impact of δ on velocity profile

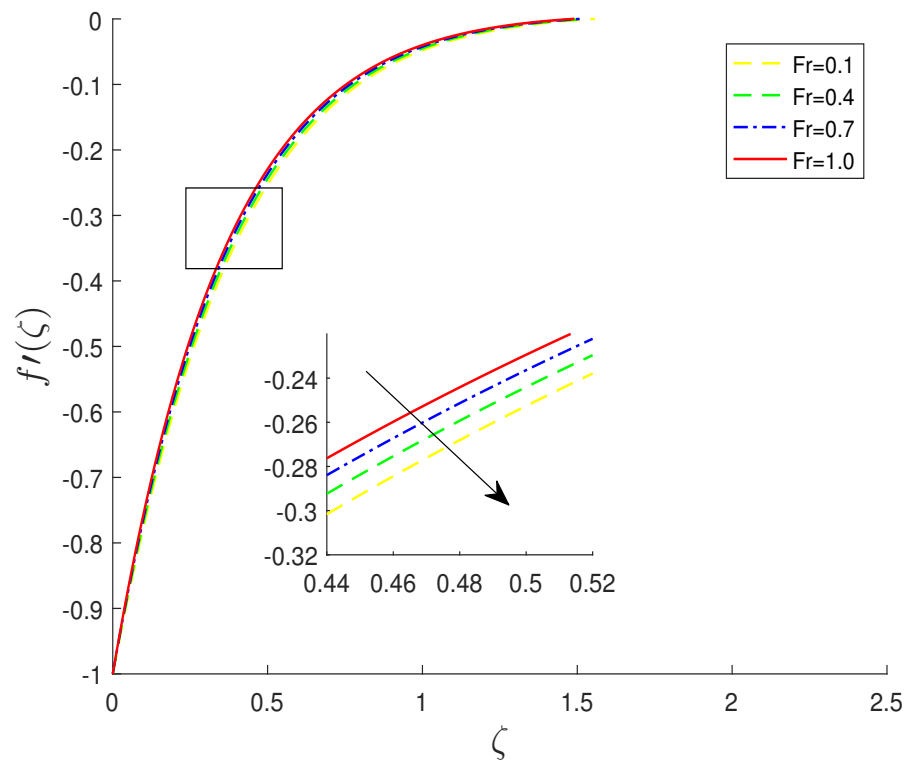


FIGURE 3.8: Impact of Fr on velocity profile

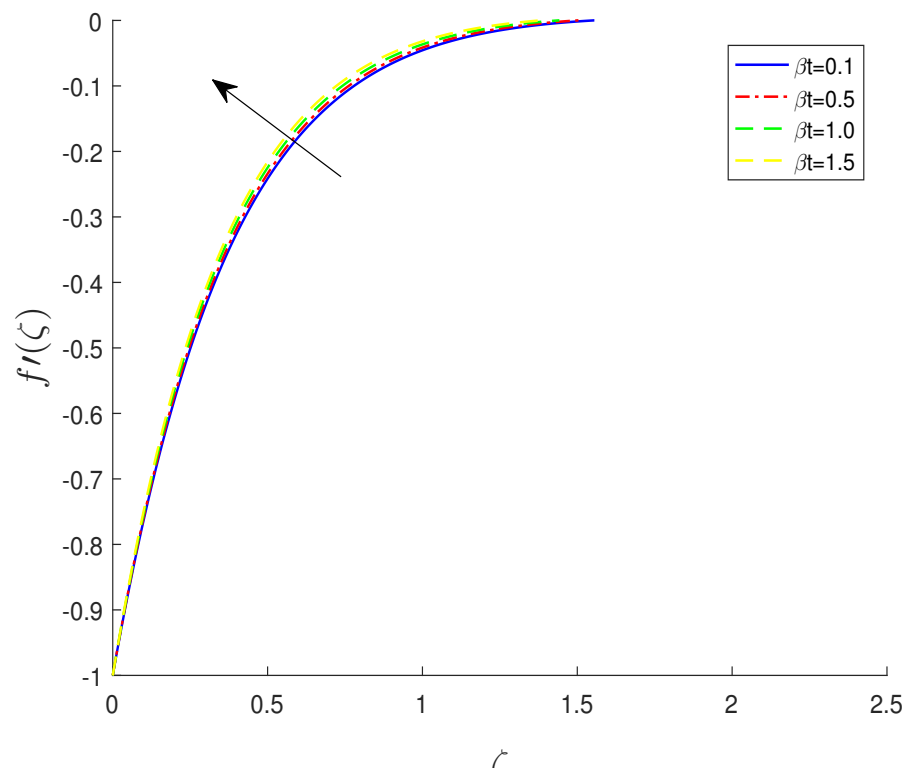


FIGURE 3.9: Impact of β_t on velocity

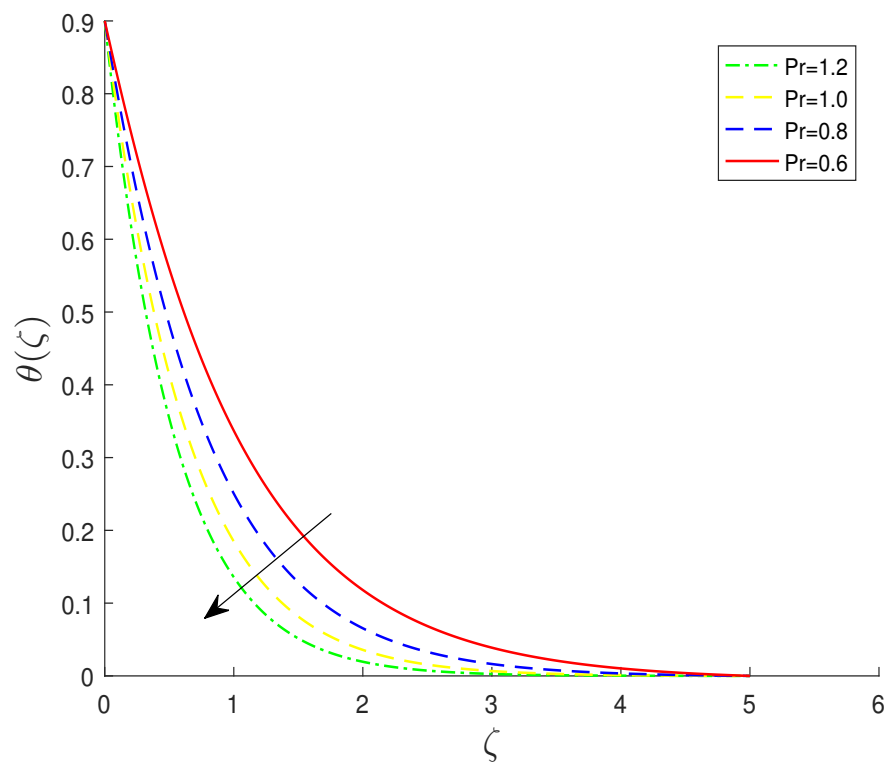


FIGURE 3.10: Impact of Pr on temperature profile

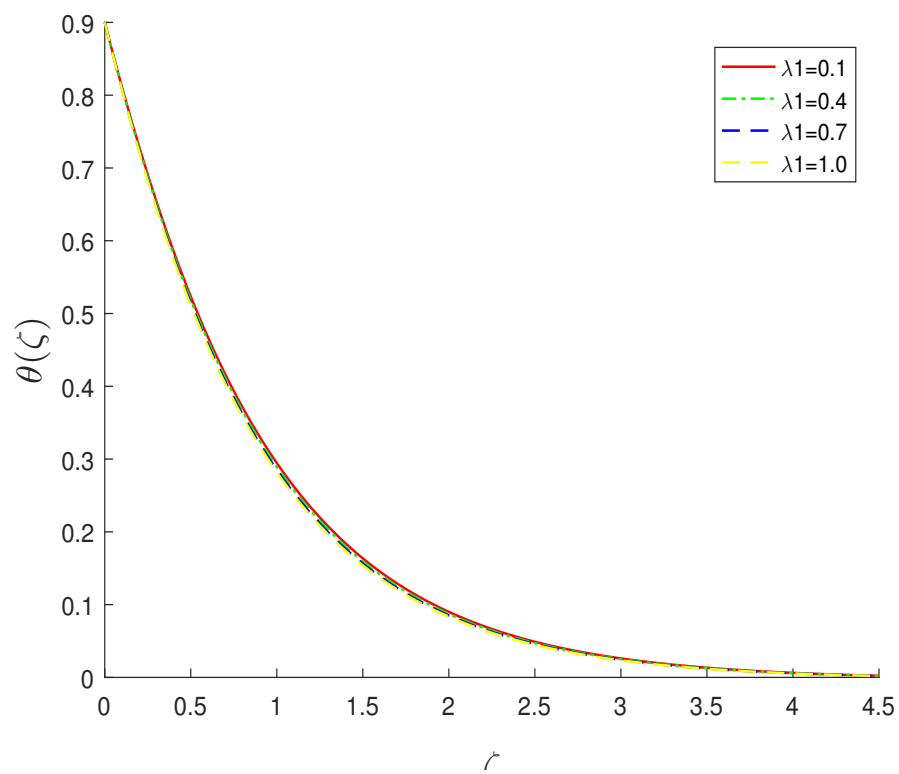


FIGURE 3.11: Impact of λ_1 on temperature

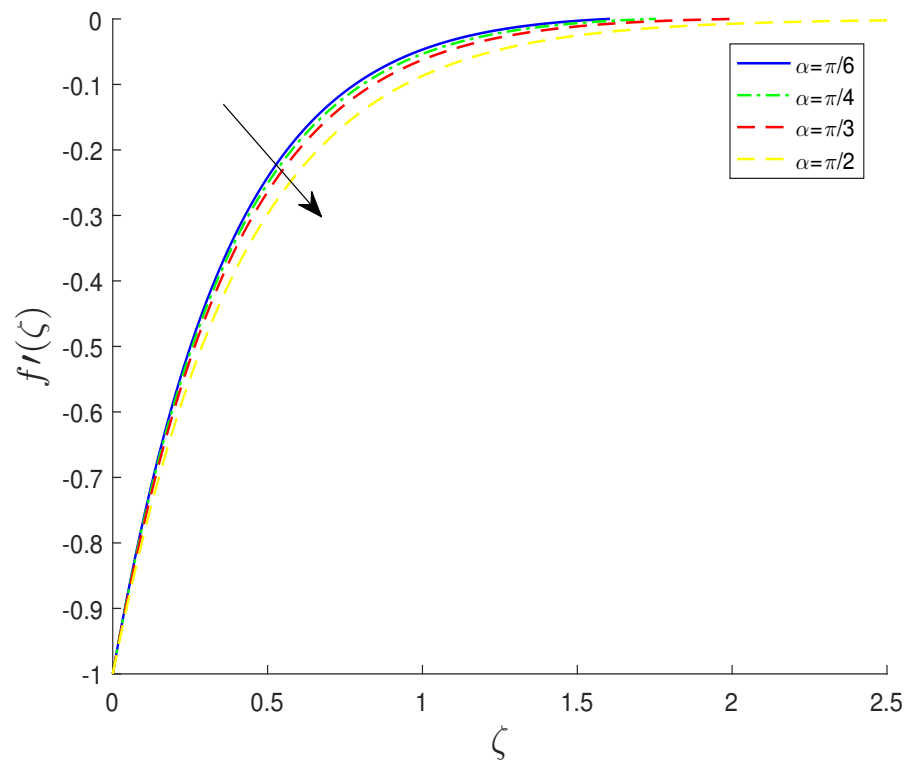


FIGURE 3.12: Impact of α on velocity

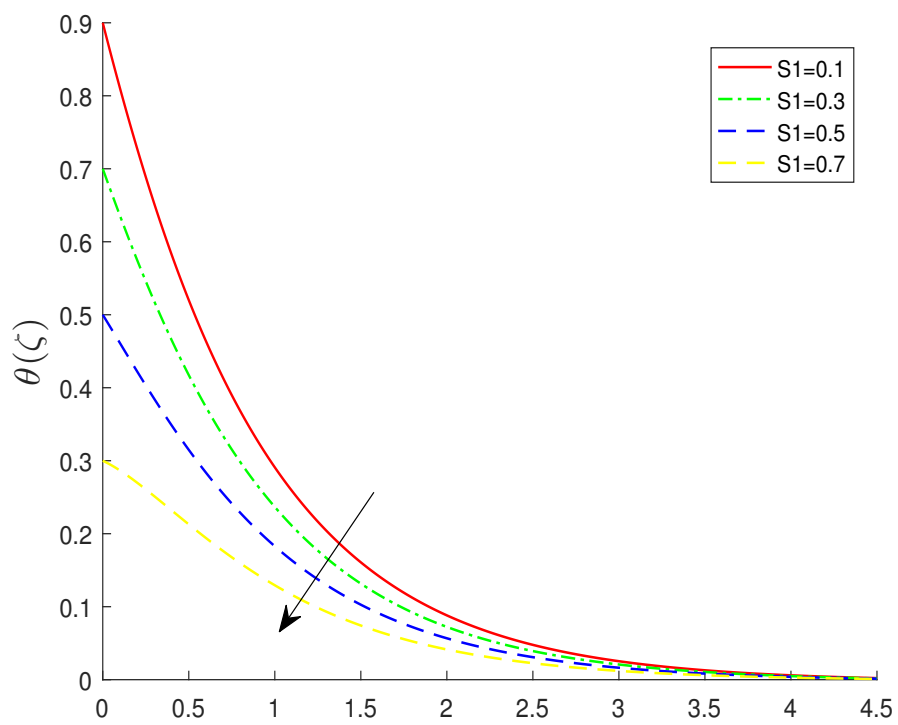


FIGURE 3.13: Impact of S_1 on temperature profile

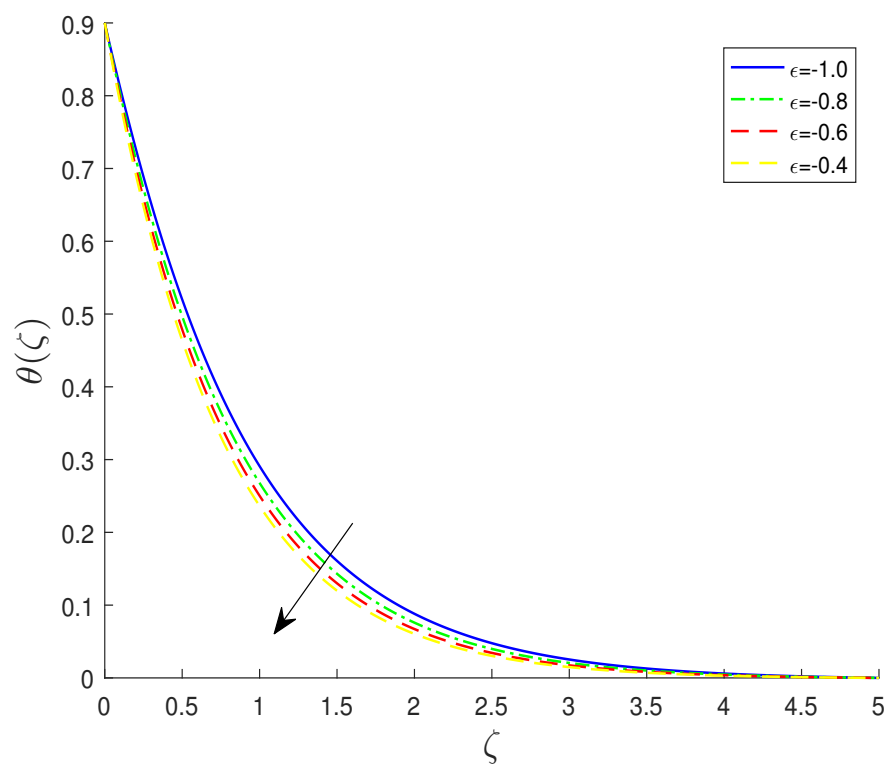


FIGURE 3.14: Impact of c on temperature

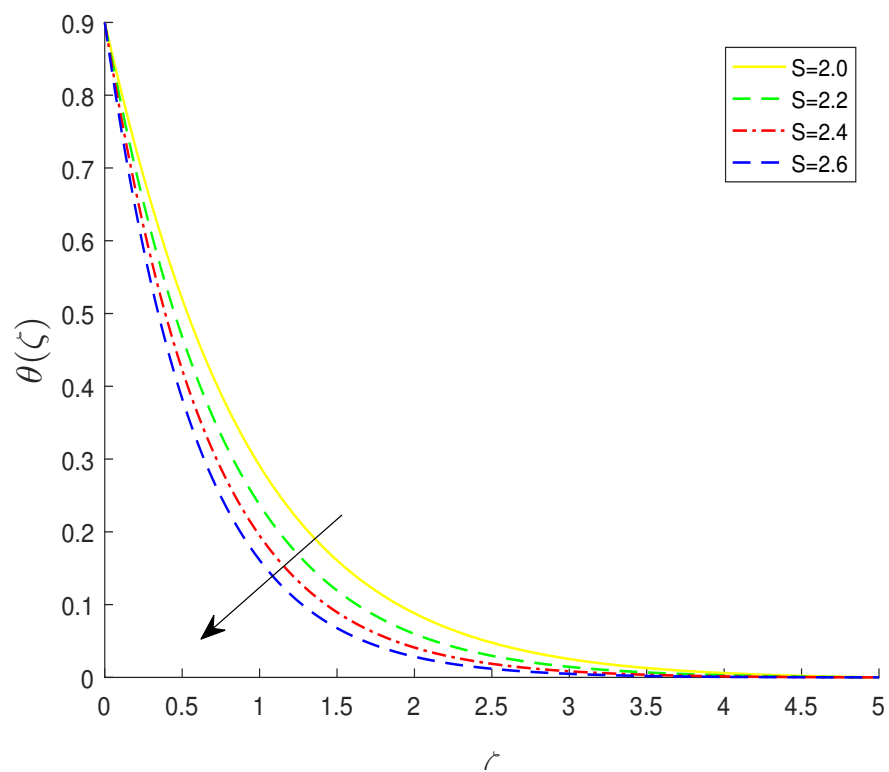
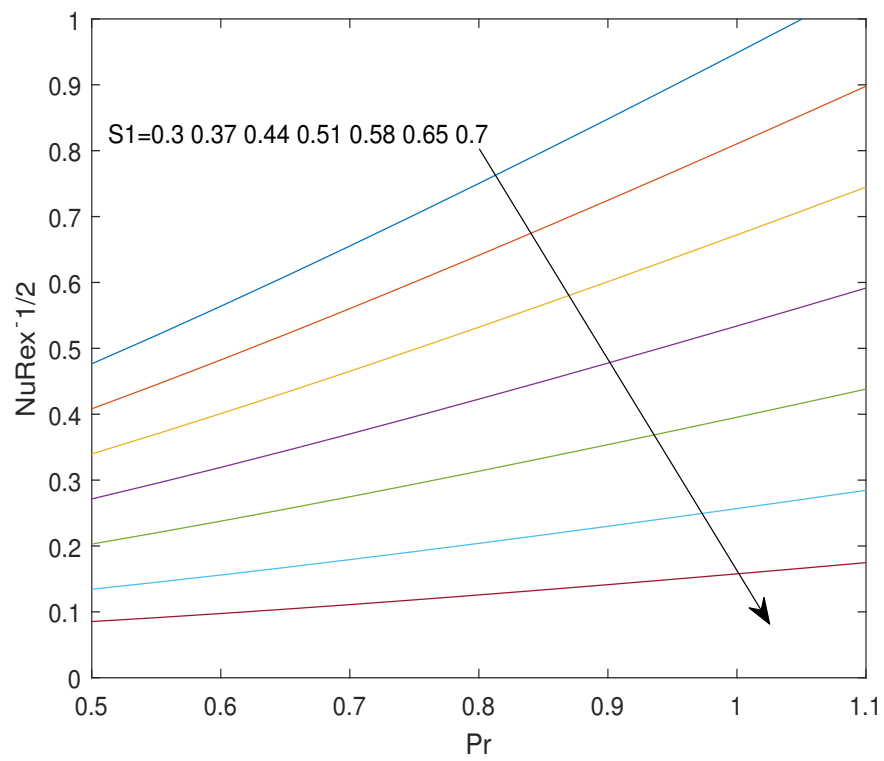


FIGURE 3.15: Impact of S on temperature

FIGURE 3.16: Impact of Pr and S_1 on Nusselt number

Chapter 4

Cattaneo-Christov Model For a Non-Newtonian Flow Over Stratified Stretching/Shrinking Inclined Sheet

4.1 Introduction

In this chapter, an extension of the model discussed in Chapter 3, has been proposed and analyzed. Momentum equation remains the same as that in Chapter 3 and the Cattaneo-Christov heat flux is added in the temperature equation.

Furthermore, the concentration equation is extended by adding Cattaneo-Christov mass flux and chemical reaction. The given nonlinear partial differential equations are converted into dimensionless form by utilizing the same similarity transformation. In order to solve the ordinary differential equations, shooting method is applied. For numerical computation, the computational software MATLAB is adopted. Lastly, the numerical results are discussed for different parameters affecting velocity, temperature and concentration profiles and these results are presented through tables and graphs.

4.2 Mathematical Modeling

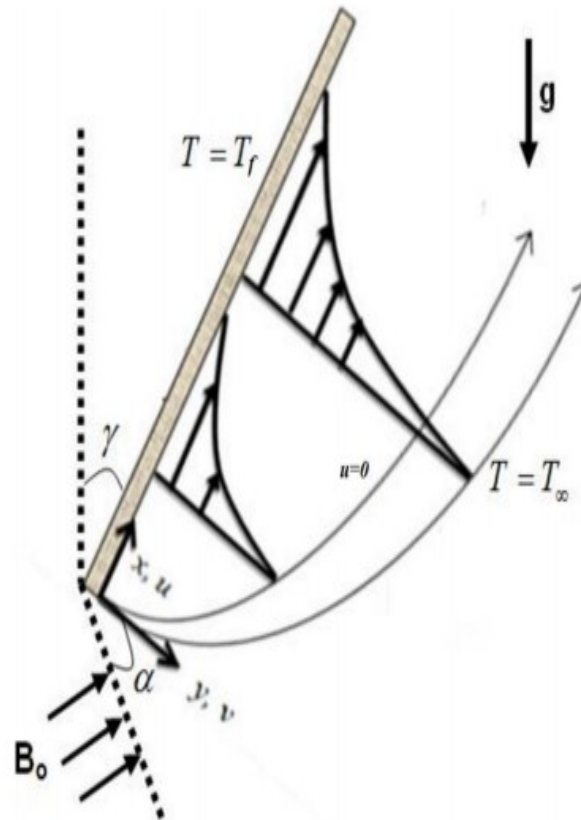


FIGURE 4.1: Geometry for the flow under discussion.

It has been aimed to examine a 2D upper-convected Maxwell fluid flow over shrinking sheet with aligned magnetic field.

The inclination angle is α , B_0 is the aligned magnetic field with angle γ and velocity $u_w = ax$ has been considered. The temperature on the wall is $T_f = T_0 + a_1x$

and $T_\infty = T_0 + d_1x$ is the temperature far from the wall. In addition, Cattaneo-

Cristove double diffusion model and the concentration of fluid is also examined

with the assistance of concentration equation under the effect of chemical reaction

By considering the above assumptions, the governing partial differential equations are:

$$\frac{\partial u}{\partial x} + \frac{\partial v}{\partial y} = 0, \quad (4.1)$$

$$u \frac{\partial u}{\partial x} + v \frac{\partial u}{\partial y} + \lambda \left(u^2 \frac{\partial^2 u}{\partial x^2} + v^2 \frac{\partial^2 u}{\partial y^2} + 2uv \frac{\partial^2 u}{\partial x \partial y} \right) = \nu \frac{\partial^2 u}{\partial y^2} \quad (4.2)$$

$$\begin{aligned} & - \frac{\sigma B_o^2}{\rho} \sin^2(\gamma) \left(u + \lambda v \frac{\partial u}{\partial y} \right) + g(\beta_1(T - T_\infty) + \beta_2(T - T_\infty)^2) \cos(\alpha) - \frac{v}{k} u - F u^2, \\ & u \frac{\partial T}{\partial x} + v \frac{\partial T}{\partial y} + \lambda \left(\left(u \frac{\partial u}{\partial x} + v \frac{\partial u}{\partial y} \right) \frac{\partial T}{\partial x} + \left(u \frac{\partial v}{\partial x} + v \frac{\partial v}{\partial y} \right) \frac{\partial T}{\partial y} + u^2 \frac{\partial^2 T}{\partial x^2} + v^2 \frac{\partial^2 T}{\partial y^2} \right. \\ & \left. + 2uv \frac{\partial^2 T}{\partial x \partial y} \right) = \frac{k}{\rho c_p} \frac{\partial^2 T}{\partial y^2}, \end{aligned} \quad (4.3)$$

$$\begin{aligned} & u \frac{\partial C}{\partial x} + v \frac{\partial C}{\partial y} + \delta \left(\left(u \frac{\partial u}{\partial x} + v \frac{\partial u}{\partial y} \right) \frac{\partial C}{\partial x} + \left(u \frac{\partial v}{\partial x} + v \frac{\partial v}{\partial y} \right) \frac{\partial C}{\partial y} + u^2 \frac{\partial^2 C}{\partial x^2} + v^2 \frac{\partial^2 C}{\partial y^2} \right. \\ & \left. + 2uv \frac{\partial^2 C}{\partial x \partial y} \right) = D_B \left(\frac{\partial^2 C}{\partial x^2} + \frac{\partial^2 C}{\partial y^2} \right) + D_T \left(\frac{\partial^2 T}{\partial x^2} + \frac{\partial^2 T}{\partial y^2} \right) - R(C - C_\infty). \end{aligned} \quad (4.4)$$

The associated BCs have been taken as:

$$\left. \begin{aligned} & u = \epsilon u_w(x), \quad v = v_0, \quad T = T_f = T_0 + a_1 x, \quad \phi = 1, \quad \text{at } y = 0, \\ & u \rightarrow 0, \quad T \rightarrow T_\infty = T_o + d_1 x, \quad \phi \rightarrow 0, \quad \text{as } y \rightarrow \infty. \end{aligned} \right\} \quad (4.5)$$

Following similarity transformation has been used to convert the partial differential equations (4.1)-(4.4) into a system of ordinary differential equations .

$$\left. \begin{aligned} & \omega(x, y) = \sqrt{\nu x u_w(x)}, \quad f(\xi) = \sqrt{a \nu} x f(\xi), \quad \theta(\xi) = \frac{T - T_\infty}{T_f - T_o}, \\ & \xi = \sqrt{\frac{u_w(x)}{\nu x}} y = \left(\frac{a}{\nu} \right)^{\frac{1}{2}} y, \quad \phi(\xi) = \frac{C - C_\infty}{C_w - C_\infty}. \end{aligned} \right\} \quad (4.6)$$

where ω denotes the stream function, ξ denotes the similarity variable, f' , θ and ϕ are the dimensionless velocity, temperature and concentration. The detailed procedure for the conversion of (4.1) is discussed in Chapter 3. The complete procedure for the conversion of (4.2) discussed in Chapter 3.

For the non-dimensional form of (4.3) the following procedure is adopted.

$$\begin{aligned}\frac{\partial^2 T}{\partial x^2} &= 0, \\ \frac{\partial^2 T}{\partial x \partial y} &= a_1 \sqrt{\frac{a}{\nu}} \theta'.\end{aligned}$$

Now, use the above derivatives to get the non-dimensional form of left hand side of (4.3).

$$\begin{aligned}u \frac{\partial T}{\partial x} + v \frac{\partial T}{\partial y} + \lambda \left(\left(u \frac{\partial u}{\partial x} + v \frac{\partial u}{\partial y} \right) \frac{\partial T}{\partial x} + \left(u \frac{\partial v}{\partial x} + v \frac{\partial v}{\partial y} \right) \frac{\partial T}{\partial y} + u^2 \frac{\partial^2 T}{\partial x^2} + v^2 \frac{\partial^2 T}{\partial y^2} \right. \\ \left. + 2uv \frac{\partial^2 T}{\partial x \partial y} \right) = \theta f' + S_1 \left(f' + \lambda_2 f'^2 - \lambda_2 f f'' \right) \\ + \lambda_2 \left(f'^2 \theta - f f'' \theta - f f' \theta' \right).\end{aligned}\quad (4.7)$$

Now, convert the right hand side of (4.3) into the dimensionless form.

$$\frac{k}{\rho c_p} \frac{\partial^2 T}{\partial y^2} = \left(\frac{1}{Pr} - \lambda_2 f^2 \right) \theta''.\quad (4.8)$$

Comparing (4.7) and (4.8), we get the dimensionless form of (4.3), as follows.

$$\theta f' + S_1 \left(f' + \lambda_2 f'^2 - \lambda_2 f f'' \right) + \lambda_2 \left(f'^2 \theta - f f'' \theta - f f' \theta' \right) = \left(\frac{1}{Pr} - \lambda_2 f^2 \right) \theta''.\quad (4.9)$$

For the conversion of (4.4), we do the following steps:

$$\begin{aligned}\phi(\xi) &= \frac{C - C_\infty}{C_w - C_\infty}. \\ C &= \phi(C_w - C_\infty) + C_\infty. \\ \frac{\partial C}{\partial x} &= 0. \\ \frac{\partial^2 C}{\partial x^2} &= 0. \\ \frac{\partial C}{\partial y} &= (C_w - C_\infty) \phi'(\xi) \sqrt{\frac{a}{\nu}}. \\ \frac{\partial^2 C}{\partial^2 y} &= \frac{a}{\nu} (C_w - C_\infty) \phi''.\end{aligned}$$

To get dimensionless form of left hand side of (4.4), we have following steps:

$$\begin{aligned}
 & u \frac{\partial C}{\partial x} + v \frac{\partial C}{\partial y} + \delta \left(\left(u \frac{\partial u}{\partial x} + v \frac{\partial u}{\partial y} \right) \frac{\partial C}{\partial x} + \left(u \frac{\partial v}{\partial x} + v \frac{\partial v}{\partial y} \right) \frac{\partial C}{\partial y} \right. \\
 & \quad \left. + u^2 \frac{\partial^2 C}{\partial x^2} + v^2 \frac{\partial^2 C}{\partial y^2} + 2uv \frac{\partial^2 C}{\partial x \partial y} \right) \\
 & = -\sqrt{a\nu}(C_w - C_\infty)\phi' \sqrt{\frac{a}{\nu}} + \delta \left((-\sqrt{a\nu})(-af')(C_w - C_\infty)\phi' \sqrt{\frac{a}{\nu}} \right) \\
 & \quad + (-\sqrt{a\nu}f)^2 \left(\frac{a}{\nu}(C_w - C_\infty)\phi'' \right) \\
 & = \left(C_w - C_\infty \right) \left(-af\phi' + \delta \left(a^2 f f' \phi' + a^2 f^2 \phi'' \right) \right). \tag{4.10}
 \end{aligned}$$

To get the non-dimensional form of right hand side of (4.4), we have following steps:

$$\begin{aligned}
 & D_B \left(\frac{\partial^2 C}{\partial x^2} + \frac{\partial^2 C}{\partial y^2} \right) + D_T \left(\frac{\partial^2 T}{\partial x^2} + \frac{\partial^2 T}{\partial y^2} \right) - R(C - C_\infty) \\
 & = D_B \left(\frac{a}{\nu}(C_w - C_\infty)\phi'' \right) + D_T \left(\frac{a}{\nu}(T_w - T_\infty)\theta'' \right) - R(C_w - C_\infty)\phi \\
 & = \left(C_w - C_\infty \right) \left(D_B \left(\frac{a}{\nu} \right) \phi'' + D_T \left(\frac{a}{\nu} \right) \left(\frac{T_w - T_\infty}{C_w - C_\infty} \right) \theta'' - R\phi \right). \tag{4.11}
 \end{aligned}$$

Comparing (4.10) and (4.11), we get the dimensionless form of governing mathematical model is as follow.

$$\begin{aligned}
 & (C_w - C_\infty)(-af\phi' + \delta(a^2 f f' \phi' + a^2 f^2 \phi'')) \\
 & = \left(C_w - C_\infty \right) \left(D_B \left(\frac{a}{\nu} \right) \phi'' + D_T \left(\frac{a}{\nu} \right) \left(\frac{T_w - T_\infty}{C_w - C_\infty} \right) \theta'' - R\phi \right). \\
 & \Rightarrow -af\phi' + \delta(a^2 f f' \phi' + a^2 f^2 \phi'') \\
 & = D_B \left(\frac{a}{\nu} \right) \phi'' + D_T \left(\frac{a}{\nu} \right) \left(\frac{T_w - T_\infty}{C_w - C_\infty} \right) \theta'' - R\phi \\
 & \Rightarrow -f\phi' + \delta a(f f' \phi' + f^2 \phi'') \\
 & = \frac{D_B \phi''}{\nu} + D_T \left(\frac{a}{\nu} \right) \left(\frac{T_w - T_\infty}{C_w - C_\infty} \right) \theta'' - \frac{R}{a} \phi \\
 & \Rightarrow -f\phi' + \lambda_3(f f' \phi' + f^2 \phi'') = \frac{1}{S_c} \phi'' + S_o \theta'' - \epsilon \phi. \tag{4.12}
 \end{aligned}$$

BCs are converted into the dimensionless form through the following steps:

$$\begin{aligned}
 & \bullet \quad u = \epsilon u_w && \text{at } y = 0. \\
 & \Rightarrow ax f'(\xi) = \epsilon ax && \text{at } \xi = 0. \\
 & \Rightarrow f'(\xi) = \epsilon && \text{at } \xi = 0. \\
 & \Rightarrow f'(0) = \epsilon \\
 \\
 & \bullet \quad v = v_0 && \text{at } y = 0. \\
 & \Rightarrow -\sqrt{av} f = -\sqrt{av} f(0) && \text{at } \xi = 0. \\
 & \Rightarrow f(\xi) = f(0) \\
 \\
 & \bullet \quad T = T_f = T_0 + a_1 x && \text{at } y = 0. \\
 & \Rightarrow \theta(T_w - T_\infty) + T_\infty = T_0 + a_1 x && \text{at } \xi = 0. \\
 & \Rightarrow \theta(T_0 + a_1 x - T_0 - d_1 x) + T_0 + d_1 x = T_0 + a_1 x && \text{at } \xi = 0. \\
 & \Rightarrow \theta(a_1 x - d_1 x) + d_1 x = a_1 x && \text{at } \xi = 0. \\
 & \Rightarrow \theta(0)(a_1 - d_1)x = (a_1 - d_1)x && \text{at } \xi = 0. \\
 \\
 & \bullet \quad C = C_w && \text{at } y = 0. \\
 & \Rightarrow (C_w - C_\infty)\phi + C_\infty = C_w && \text{at } \xi = 0. \\
 & \Rightarrow (C_w - C_\infty)\phi(\xi) = (C_w - C_\infty) && \text{at } \xi = 0. \\
 & \Rightarrow \phi(\xi) = 1 && \text{at } \xi = 0. \\
 & \Rightarrow \phi(0) = 1 \\
 \\
 & \bullet \quad u \rightarrow 0 && \text{as } y \rightarrow 0. \text{ as} \\
 & \Rightarrow ax f' \rightarrow 0 && \xi \rightarrow \infty. \text{ as } \xi \\
 & \Rightarrow f' \rightarrow 0 && \rightarrow \infty. \\
 & \Rightarrow f'(\infty) \rightarrow 0 && \text{as } \xi \rightarrow \infty.
 \end{aligned}$$

$$\begin{aligned}
 &\bullet T \rightarrow T_\infty = T_0 + d_1x && \text{as } y \rightarrow \infty. \\
 &\Rightarrow \theta(T_w - T_\infty) + T_\infty \rightarrow T_0 + d_1x. \\
 &\Rightarrow \theta(T_0 + a_1x - T_0 - d_1x) + (T_0 + d_1x) \rightarrow T_0 + d_1x. \\
 &\Rightarrow \theta(a_1x - d_1x) \rightarrow 0. \\
 &\Rightarrow \theta \rightarrow 0 && \text{as } \xi \rightarrow \infty. \\
 &\Rightarrow \theta(\infty) \rightarrow 0 && \text{as } \xi \rightarrow \infty. \\
 \\
 &\bullet C \rightarrow C_\infty && \text{as } y \rightarrow \infty. \\
 &\Rightarrow C_\infty + \phi(\xi)(C_w - C_\infty) \rightarrow C_\infty && \text{as } \xi \rightarrow \infty. \\
 &\Rightarrow \phi(C_w - C_\infty) \rightarrow 0 && \text{as } \xi \rightarrow \infty. \\
 &\Rightarrow \phi \rightarrow 0 && \text{as } \xi \rightarrow \infty.
 \end{aligned}$$

Dimensionless form of the BCs:

$$\left. \begin{aligned}
 f'(0) = \epsilon, \quad f(0) = S, \quad \theta(0) = 1 - S_1, \quad \phi(0) = 1, \quad \text{at } \xi = 0 \\
 f'(\xi) \rightarrow 0, \quad \theta(\xi) \rightarrow 0, \quad \phi(\xi) \rightarrow 0 \quad \text{as } \xi \rightarrow \infty.
 \end{aligned} \right\} \quad (4.13)$$

Parameters used in the equations are:

$$\begin{aligned}
 \delta &= \frac{Gr_x}{Re_x^2}, \quad \beta_t = \frac{\beta_2(T_f - T_0)}{\beta_1}, \quad \lambda_1 = \frac{\nu}{Ka}, \quad Fr = \frac{C_p}{\sqrt{K}}x, \\
 Gr_x &= g\beta_1 \frac{(T_f - T_0)x^3}{\nu^2}, \quad Re_x = \frac{xu_w}{\nu}, \quad u_w = ax. \quad Pr = \frac{\mu c_p}{k}, \\
 \beta &= \lambda a, \quad M = \sigma \frac{\beta_0^2}{\rho a}, \quad \mu = \rho\nu, \quad S_1 = \frac{d_1}{a_1}, \\
 \lambda_2 &= \delta a, \quad S_c = \frac{\nu}{D_B}, \quad S_0 = \frac{D_T}{\nu} \left(\frac{T_w - T_\infty}{C_w - C_\infty} \right), \\
 \epsilon &= \frac{R}{a}, \quad \lambda_2 = \lambda a, \quad \lambda_3 = \delta a.
 \end{aligned}$$

The sherwood number is expressed as:

$$Sh_x = \frac{xq_m}{D_B(C_w - C_\infty)}. \quad (4.14)$$

Now for non-dimensional form of sherwood number ,following steps are taken:

$$\begin{aligned}
 q_m &= -D_B \left(\frac{\partial T}{\partial y} \right)_{y=0} & (4.15) \\
 Sh_x &= \frac{x - D_B \left(\frac{\partial T}{\partial y} \right)_{y=0}}{D_B (C_w - C_\infty)} \\
 &= -x ((C_w - C_\infty) \sqrt{\frac{a}{\nu}} \phi'(0)) \\
 &= -\sqrt{\frac{ax^2}{\nu}} \phi'(0) \\
 &= -\sqrt{Re_x} \phi'(0) \\
 \Rightarrow \frac{sh_x}{\sqrt{Re_x}} &= \phi'(0).
 \end{aligned}$$

$$\text{where } Re = \frac{xu_x(x)}{\nu_f}.$$

4.3 Solution Methodology

In this section, shooting method has been used to obtain the approximate solution of the ordinary differential equations (3.27), (4.9) and (4.12) along with the boundary conditions (4.13). Firstly, we solve the coupled ordinary differential equations (3.27) and (4.9).

Let us consider the following notations:

$$\begin{aligned}
 f &= z_1, & f' &= z'_1 = z_2, & f'' &= z''_1 = z'_2 = z_3, & f''' &= z'_3, \\
 \theta &= z_4, & \theta' &= z'_4 = z_5, & \theta'' &= z_5.
 \end{aligned}$$

Convert equation into first order ODEs by using notations:

$$\begin{aligned}
 z'_1 &= z_2, & z_1(0) &= S, \\
 z'_2 &= z_3, & z_2(0) &= c,
 \end{aligned}$$

$$\begin{aligned}
 z_3' &= \left(-z_1 z_3 - 2\beta z_1 z_2 z_3 - M \sin^2(\gamma)[\beta z_1 z_3 - z_2] - \delta(1 + \beta_t z_4) z_4 \cos(\alpha) \right. \\
 &\quad \left. + \lambda_1 z_2 + (1 + Fr) z_2^2 \right) (1 - \beta z_1^2)^{-1}, & z_3(0) &= MC_1, \\
 z_4' &= z_5, & z_4(0) &= 1 - S_1, \\
 z_5' &= \left(\frac{1}{Pr} - \lambda_2 z_1^2 \right)^{-1} \left(z_2 z_5 + S_1(z_2 + \lambda_2 z_2^2 - \lambda_2 z_1 z_3) + \lambda_2(z_2^2 z_4 - z_1 z_3 z_4 - z_1 z_2 z_5) \right), \\
 & & z_5(0) &= MC_2.
 \end{aligned}$$

In the above IVP, the missing conditions MC_1 and MC_2 , are chosen to satisfy the following relation.

$$(z_2(MC_1, MC_2))_{\xi=\xi_\infty} = 0, \quad (z_4(MC_1, MC_2))_{\xi=\xi_\infty} = 0.$$

Now apply Newton's method to solve the above algebraic equations, by using following formula.

$$\begin{bmatrix} MC_1 \\ MC_2 \end{bmatrix}_{n+1} = \begin{bmatrix} MC_1 \\ MC_2 \end{bmatrix}_n - \begin{bmatrix} \frac{\partial z_2}{\partial MC_1} & \frac{\partial z_2}{\partial MC_2} \\ \frac{\partial z_4}{\partial MC_1} & \frac{\partial z_4}{\partial MC_2} \end{bmatrix}_n^{-1} \begin{bmatrix} z_2 \\ z_4 \end{bmatrix}_n.$$

Now introduce the following new notations:

$$\begin{aligned}
 \frac{\partial z_1}{\partial MC_1} &= z_6, & \frac{\partial z_2}{\partial MC_1} &= z_7, & \frac{\partial z_3}{\partial MC_1} &= z_8, & \frac{\partial z_4}{\partial MC_1} &= z_9, & \frac{\partial z_5}{\partial MC_1} &= z_{10}, \\
 \frac{\partial z_1}{\partial MC_2} &= z_{11}, & \frac{\partial z_2}{\partial MC_2} &= z_{12}, & \frac{\partial z_3}{\partial MC_2} &= z_{13}, & \frac{\partial z_4}{\partial MC_2} &= z_{14}, & \frac{\partial z_5}{\partial MC_2} &= z_{15}.
 \end{aligned}$$

Newton iterative scheme get form by using new notations

$$\begin{bmatrix} MC_1 \\ MC_2 \end{bmatrix}_{n+1} = \begin{bmatrix} MC_1 \\ MC_2 \end{bmatrix}_n - \begin{bmatrix} z_7 & z_{12} \\ z_9 & z_{14} \end{bmatrix}_n^{-1} \begin{bmatrix} z_2 \\ z_4 \end{bmatrix}_n$$

The above itrative process will be continued untill the following criteria is fulfilled.

$$max\{|z_2(\xi_\infty, MC_1 n, MC_2 n)|, |z_4(\xi_\infty, MC_1 n, MC_2 n)|\} < \chi,$$

where χ has been taken as 10^{-5} .

Differentiating the last system of first order ODEs w.r.t MC_1 and MC_2 , we get:

$$\begin{aligned}
z'_6 &= z_7, & z_6(0) &= 0, \\
z'_7 &= z_8, & z_7(0) &= 0, \\
z'_8 &= (1 - \beta z_1^2)^{-1} (-z_1 z_8 - z_6 z_3 - 2\beta z_1 z_2 z_8 - 2\beta z_1 z_7 z_3 - 2\beta z_6 z_2 z_3 \\
&\quad - M \sin^2(\gamma)(\beta z_1 z_8 + \beta z_6 z_3 - z_7) - \delta(1 + \beta_t z_9) z_4 \cos(\alpha) \\
&\quad - \delta(1 + \beta_t z_4) z_9 \cos(\alpha) + \lambda_1 z_7 + 2z_2 z_7(1 + Fr)) \\
&\quad + (-z_1 z_3 - 2\beta z_1 z_2 z_3 - M \sin^2(\gamma)(\beta z_1 z_3 - z_2) \\
&\quad - \delta(1 + \beta_t z_4) z_4 \cos(\alpha) - \lambda_1 z_2 + (1 + Fr) z_2^2) ((1 - \beta z_1^2)^{-2} (2\beta z_1 z_6)), \\
& & z_8(0) &= 1, \\
z'_9 &= z_{10}, & z_9(0) &= 0, \\
z'_{10} &= \left(\frac{1}{Pr} - \lambda_2 z_1^2 \right)^{-2} (2\lambda_2 z_1 z_6) (z_2 z_5 + S_1(z_2 + \lambda_2 z_2^2 - \lambda_2 z_1 z_3) \\
&\quad + \lambda_2(z_2^2 z_4 - z_1 z_3 z_4 - z_1 z_2 z_5)) + \left(\frac{1}{Pr} - \lambda_2 z_1^2 \right)^{-1} (z_7 z_5 + z_2 z_{10} \\
&\quad + S_1(z_7 + 2\lambda_2 z_2 z_7 - \lambda_2(z_6 z_3 + z_1 z_8)) + \lambda_2(2z_2 z_4 z_7 + z_2^2 z_9 - z_6 z_3 z_4 \\
&\quad - z_1 z_8 z_4 - z_1 z_3 z_9 - z_6 z_2 z_5 - z_1 z_7 z_5 - z_1 z_2 z_{10})), \\
& & z_{10}(0) &= 0, \\
z'_{11} &= z_{12}, & z_{11}(0) &= 0, \\
z'_{12} &= z_{13}, & z_{12}(0) &= 0, \\
z'_{13} &= ((1 - \beta z_1^2)^{-1}) (-z_1 z_{13} - z_{11} z_3 - 2\beta z_1 z_2 z_{13} - 2\beta z_1 z_{12} z_3 - 2\beta z_{11} z_2 z_3 \\
&\quad - M \sin^2(\gamma)(\beta z_1 z_{13} + \beta z_{11} z_3 - z_{12}) - \delta(1 + \beta_t z_{14}) z_4 \cos(\alpha) \\
&\quad - \delta(1 + \beta_t z_4) z_{14} \cos(\alpha) + \lambda_1 z_{12} + 2z_2 z_{12}(1 + Fr)) \\
&\quad + (-z_1 z_3 - 2\beta z_1 z_2 z_3 - M \sin^2(\gamma)(\beta z_1 z_3 - z_2) \\
&\quad - \delta(1 + \beta_t z_4) z_4 \cos(\alpha) + \lambda_1 z_2 + (1 + Fr) z_2^2) ((1 - \beta z_1^2)^{-2} (2\beta z_1 z_{11})), \\
& & z_{13}(0) &= 0, \\
z'_{14} &= z_{15}, & z_{14}(0) &= 0,
\end{aligned}$$

$$\begin{aligned}
 z'_{10} = & \left(\frac{1}{Pr} - \lambda_2 z_1^2 \right)^{-2} (2\lambda_2 z_1 z_{11})(z_2 z_5 + S_1(z_2 + \lambda_2 z_2^2 - \lambda_2 z_1 z_3)) \\
 & + \lambda_2(z_2^2 z_4 - z_1 z_3 z_4 - z_1 z_2 z_5) + \left(\frac{1}{Pr} - \lambda_2 z_1^2 \right)^{-1} (z_{12} z_5 + z_2 z_{15} \\
 & + S_1(z_{12} + 2\lambda_2 z_2 z_{12} - \lambda_2(z_{11} z_3 + z_1 z_{13})) + \lambda_2(2z_2 z_4 z_{12} + z_2^2 z_{14} \\
 & - z_{11} z_3 z_4 - z_1 z_{13} z_4 - z_1 z_3 z_{14} - z_{11} z_2 z_5 - z_1 z_{12} z_5 - z_1 z_2 z_{15})), \\
 & z_{15}(0) = 1.
 \end{aligned}$$

Now, solve the equation (4.12). Let us consider following notations:

$$\phi = e_1, \quad \phi' = e'_1 = e_2, \quad \phi'' = e'_2.$$

Convert equations into first order ODEs by using notations:

$$\begin{aligned}
 e'_1 &= e_2, & e_1(0) &= 1, \\
 e'_2 &= \left(\frac{1}{S_c} - \lambda_3 c_1^2 \right)^{-1} \left(-c_1 e_2 + \lambda_3 c_1 c_2 e_2 - S_0 \left(\frac{-c_1 c_3 + \lambda_2 c_1 c_2 c_3}{1/Pr - \lambda_2 c_1^2} \right) + \epsilon e_1 \right), \\
 & & e_2(0) &= w.
 \end{aligned}$$

In the above IVP, the missing condition w is chosen to satisfy the following relation.

$$e_1(\xi_\infty)_w = 0$$

Now apply Newton's method to solve algebraic equations by using following formula.

$$w_{n+1} = w_n - \frac{(e_1(\xi_\infty))_{w=w_n}}{\left(\frac{\partial e_1(\xi_\infty)}{\partial w} \right)}$$

Now, introduce the following new notations:

$$\frac{\partial e_1}{\partial w} = e_3, \quad \frac{\partial e_2}{\partial w} = e_4.$$

Newton iterative scheme get form by using new notations

$$w_{n+1} = w_n - \frac{(e_1(\xi_\infty))_{w=w_n}}{(e_3(\xi_\infty))}$$

The above iterative procedure will be continued until the following criteria is fulfilled.

$$(e_1(\xi_\infty))_{w=w_n} < \chi$$

where χ has been taken 10^{-5} .

Differentiate the system of first order ODEs w.r.t w , we get

$$\begin{aligned} e_3 &= e_4, & e_3(0) &= 0, \\ e_4 &= \left(\frac{1}{S_c} - \lambda_3 c_1^2 \right)^{-1} \left(-c_1 e_4 + \lambda_3 c_1 c_2 e_4 + \epsilon e_3 \right), & e_4(0) &= 1. \end{aligned}$$

4.4 Results and Discussions

In this section, the effect of different parameters on the velocity, temperature and concentration distributions will be analyzed by using table and graph. TABLE 4.1

and TABLE 4.2 show the impact of different parameters on skin friction $(Re_x)^{\frac{1}{2}} C_f$ and local Nusselt number $(Re_x)^{-\frac{1}{2}} Nu_x$ respectively. Increasing the value of Pr , M , β , β_t , λ_1 and δ causes a gain in the skin friction $(Re_x)^{\frac{1}{2}} C_f$ and local Nusselt number $(Re_x)^{-\frac{1}{2}} Nu_x$. However Fr and S_1 have inverse relation with skin friction $(Re_x)^{\frac{1}{2}} C_f$ and local Nusselt number $(Re_x)^{-\frac{1}{2}} Nu_x$. Moreover, when γ is increased, the skin friction $(Re_x)^{\frac{1}{2}} C_f$ is decreased but an increment in the local Nusselt number $(Re_x)^{-\frac{1}{2}} Nu_x$ can be observed. Similarly when c is boosted, the in skin friction $(Re_x)^{\frac{1}{2}} C_f$ increased and local Nusselt number $(Re_x)^{-\frac{1}{2}} Nu_x$ decreased. TABLE 4.3 analyze the impact of different parameters on Sherwood number $(Re_x)^{-\frac{1}{2}} sh_x$. By

rising γ , M , β , β_t , δ , λ_2 , Sc , Sr , ϵ , Sherwood number $(Re_x)^{-\frac{1}{2}}sh_x$ is increased. But when Pr , Fr , λ_1 , S_1 , c are increased, Sherwood number $(Re_x)^{-\frac{1}{2}}sh_x$ decreased. In these tables, I_f and I_θ are the intervals from which the missing conditions can be chosen.

FIGURE 4.2 elaborates the impact of γ on velocity profile. By increasing the value of γ , the velocity profile is increased. FIGURE 4.3 shows that when β is increased, the velocity profile declined. FIGURE 4.4 indicates the effect of Fr on velocity profile. Increasing the value of Fr causes increment in velocity profile. FIGURE 4.5 observes that when α increases, velocity decreases drastically. FIGURE 4.6 shows that when δ increases, velocity is decreased. FIGURE 4.7 elaborates the impact of B_t on velocity profile. When B_t increases, velocity is increased.

FIGURE 4.8 shows the impact of δ on temperature profile. It can be observed that when δ increases, the temperature profile is increased. FIGURE 4.9 tells about the impact of Pr on the temperature profile. It can be recognised that by increasing the value of Pr , the temperature profile demolished. FIGURE 4.10 observes that when λ_1 is boosted, temperature decreases. FIGURE 4.11 shows the effect of S_1 on the temperature profile. Here by rising the value of S_1 causes an decrement in temperature profile.

FIGURE 4.12 shows that when the value ϵ is increased, concentration profile decreases. FIGURE 4.13 shows the relationship between λ_3 and concentration profile. For higher values of λ_3 reduces concentration profile. FIGURE 4.14 shows the impact of Sc on concentration. Increasing the value of Sc causes decrement in concentration profile. FIGURE 4.15 indicates that rising the value of Sr causes decline in concentration domain. FIGURE 4.16 indicates the effect of λ_2 on the concentration profile. It can be observed that when λ_2 increases, concentration profile goes up.

TABLE 4.1:

Results of $(Re_x)^{\frac{1}{2}}C_f$ for $S = 2$ and other various parameters

γ	Pr	M	β	Fr	β_t	λ_1	λ_2	S_1	δ	c	I_f	I_θ	$(Re_x)^{\frac{1}{2}}C_f$
$\frac{\pi}{6}$	0.7	1	0.1	0.3	0.5	0.3	0.3	0.1	0.2	-1	[2.0,2.5]	[-5.5,-5.0]	2.473228
$\frac{\pi}{4}$											[2.4,2.9]	[-5.5,-5.0]	2.730991
$\frac{\pi}{3}$											[2.7,3.1]	[-5.5,-5.0]	2.959223
$\frac{\pi}{2}$											[2.9,3.3]	[-5.5,-5.0]	3.167758
	0.4										[0.1,0.5]	[-0.9,-0.2]	-0.291145
	0.5										[0.1,0.5]	[-0.9,-0.5]	-0.259397
	0.6										[0.1,0.5]	[-0.9,-0.5]	-0.212756
		0									[2.0,2.5]	[-5.5,-5.0]	2.163861
		2									[2.5,2.9]	[-5.5,-5.0]	2.730994
		3									[2.6,2.9]	[-5.5,-5.0]	2.959229
			0								[1.5,1.9]	[-5.5,-5.0]	1.712874
			0.005								[1.6,1.9]	[-5.5,-5.0]	1.735966
			0.05								[1.6,1.9]	[-5.5,-5.0]	1.996800
				0							[1.9,2.3]	[-5.5,-5.0]	2.582383
				0.6							[1.9,2.3]	[-5.5,-5.0]	2.355702
				0.9							[1.9,2.3]	[-5.5,-5.0]	2.227542
					0						[2.3,2.6]	[-5.5,-5.0]	2.457678
					1.0						[2.0,2.6]	[-5.5,-5.0]	2.488740
					1.5						[2.0,2.6]	[-5.5,-5.0]	2.504217
						0.09					[2.6,2.8]	[-4.7,-4.2]	2.836244
						0.1					[2.3,2.6]	[-4.7,-4.3]	2.842350
						0.2					[2.0,2.4]	[-5.0,-4.6]	2.901979
							0.09				[2.0,2.5]	[-6.5,-6.0]	3.102011
							0.1				[2.0,2.5]	[-6.5,-6.0]	3.096768
							0.2				[2.3,2.5]	[-5.7,-5.3]	3.037842
								0.2			[2.0,2.6]	[-7.5,-6.5]	2.460423
								0.3			[2.0,2.5]	[-6.9,-6.5]	2.447942
								0.4			[2.3,2.6]	[-6.5,-6.0]	2.435804
									0		[1.6,1.9]	[-5.7,-5.2]	2.370204
									0.4		[1.9,2.3]	[-5.7,-5.3]	2.572868
									0.6		[1.9,2.3]	[-5.7,-5.3]	2.669556
										-0.4	[2.3,2.6]	[-1.9,-1.5]	2.040746
										-0.6	[2.3,2.6]	[-1.9,-1.5]	2.218710
										-0.8	[2.3,2.6]	[-2.9,-2.5]	2.364065

TABLE 4.2:

Results of $(Re_x)^{-\frac{1}{2}}Nu_x$ for for $S = 2$ and other various parameters

γ	Pr	M	β	Fr	β_t	λ_1	λ_2	S_1	δ	c	I_f	I_θ	$(Re_x)^{-\frac{1}{2}}Nu_x$
$\frac{\pi}{6}$	0.7	1	0.1	0.3	0.5	0.3	0.3	0.1	0.2	-1	[2.0,2.5]	[-5.5,-5.0]	5.861098
$\frac{\pi}{4}$											[2.4,2.9]	[-5.5,-5.0]	5.920942
$\frac{\pi}{3}$											[2.7,3.1]	[-5.5,-5.0]	5.969606
$\frac{\pi}{2}$											[2.9,3.3]	[-5.5,-5.0]	6.011046
	0.4										[0.1,0.5]	[-0.9,-0.2]	0.584707
	0.5										[0.1,0.5]	[-0.9,-0.5]	0.931997
	0.6										[0.1,0.5]	[-0.9,-0.5]	1.713615
		0									[2.0,2.5]	[-5.5,-5.0]	5.780898
		2									[2.5,2.9]	[-5.5,-5.0]	5.920943
		3									[2.6,2.9]	[-5.5,-5.0]	5.969608
			0								[1.5,1.9]	[-5.5,-5.0]	5.633143
			0.005								[1.6,1.9]	[-5.5,-5.0]	5.641548
			0.05								[1.6,1.9]	[-5.5,-5.0]	5.728825
				0							[1.9,2.3]	[-5.5,-5.0]	5.881269
				0.6							[1.9,2.3]	[-5.5,-5.0]	5.838610
				0.9							[1.9,2.3]	[-5.5,-5.0]	5.813097
					0						[2.3,2.6]	[-5.5,-5.0]	5.858799
					1.0						[2.0,2.6]	[-5.5,-5.0]	5.863386
					1.5						[2.0,2.6]	[-5.5,-5.0]	5.865664
						0.09					[2.6,2.8]	[-4.7,-4.2]	5.943639
						0.1					[2.3,2.6]	[-4.7,-4.3]	5.944954
						0.2					[2.0,2.4]	[-5.0,-4.6]	5.957651
							0.09				[2.0,2.5]	[-1.9,-1.5]	1.462495
							0.1				[2.0,2.5]	[-1.9,-1.5]	1.513975
							0.2				[2.0,2.4]	[-2.9,-2.5]	2.367066
								0.2			[2.0,2.5]	[-6.5,-6.0]	5.207551
								0.3			[2.0,2.5]	[-6.5,-6.0]	4.554608
								0.4			[2.3,2.5]	[-5.7,-5.3]	3.902265
									0		[2.0,2.6]	[-7.5,-6.5]	5.839112
									0.4		[2.0,2.5]	[-6.9,-6.5]	5.881840
									0.6		[2.3,2.6]	[-6.5,-6.0]	5.901508
										-0.4	[1.6,1.9]	[-5.7,-5.2]	6.490795
										-0.6	[1.9,2.3]	[-5.7,-5.3]	6.286028
										-0.8	[1.9,2.3]	[-5.7,-5.3]	6.076781

TABLE 4.3:

Results of $(Re_x)^{\frac{1}{2}}Sh_x$ for $S = 2$ and other various parameters

γ	Pr	M	β	Fr	β_t	λ_1	λ_2	S_1	δ	c	λ_3	S_c	S_r	ϵ	$(Re_x)^{-\frac{1}{2}}Sh_x$
$\frac{\pi}{6}$ $\frac{\pi}{4}$ $\frac{3}{\pi}$ $\frac{2}{2}$	0.7	1	0.1	0.3	0.5	0.3	0.3	0.1	0.2	-1	0.2	0.3	0.1	0.2	0.959256
															0.975188
															0.987858
															0.998420
		0.4													0.549587
		0.5													0.556657
		0.6													0.567433
			0												0.937417
			2												0.975189
			3												0.987859
				0											0.895778
				0.005											0.898154
				0.05											0.922756
					0										0.964297
					0.6										0.953602
					0.9										0.947147
						0									0.958698
						1.0									0.959809
						1.5									0.960361
							0.09								0.947206
						0.1								0.947856	
						0.2								0.953901	
							0.09							0.557339	
							0.1							0.558008	
							0.2							0.566855	
								0.2						0.958576	
								0.3						0.957905	
								0.4						0.957244	
									0					0.953470	
									0.4					0.964689	
									0.6					0.969817	
										-0.7				0.967776	
										-0.8				0.967595	
										-0.9				0.965095	
											0.1			0.857018	
											0.3			1.096633	
											0.4			1.291429	
												0.1		0.392016	
												0.2		0.641148	
												0.4		1.362916	
													0.2	1.152611	
													0.3	1.345966	
													0.4	1.539322	
													0.1	0.916263	
													0.3	0.999247	
													0.4	1.036703	

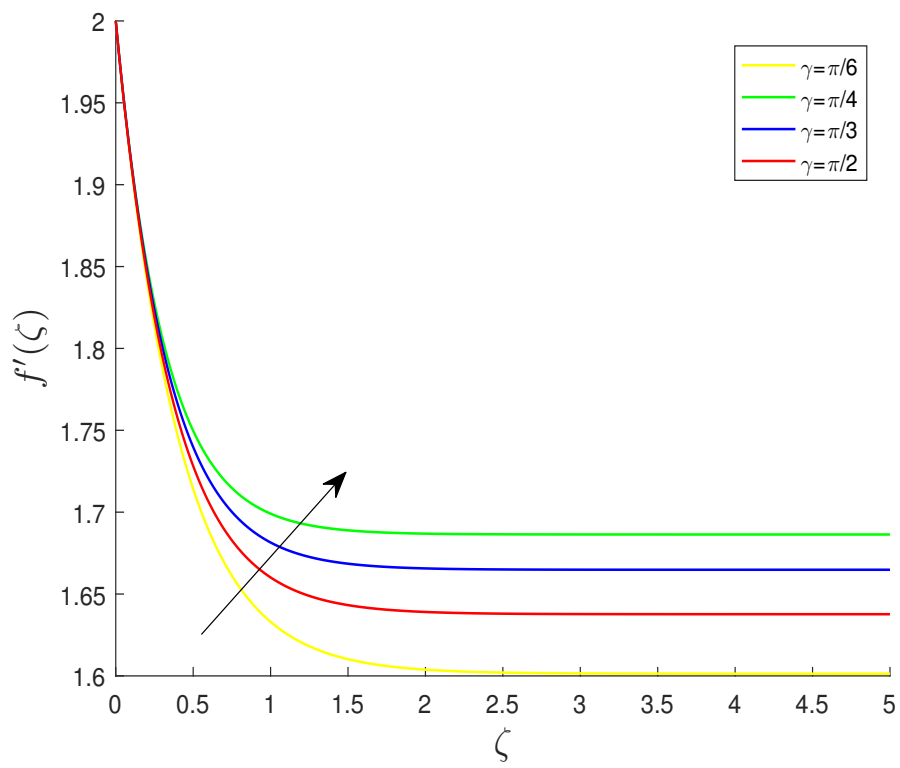


FIGURE 4.2: Impact of γ on the velocity profile.

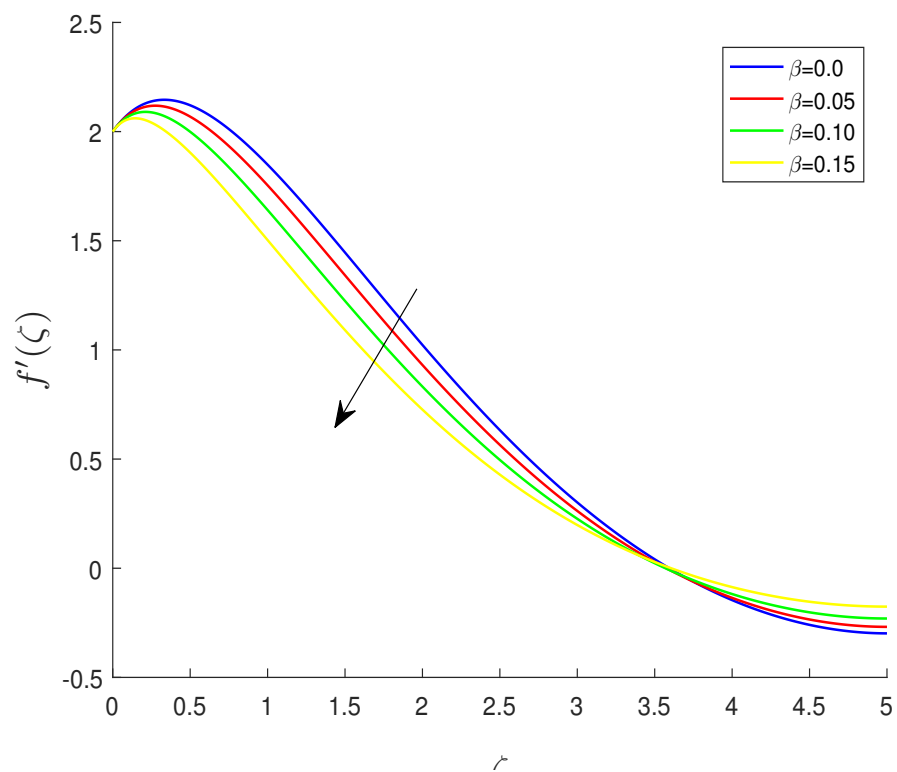


FIGURE 4.3: Impact of β on the velocity profile.

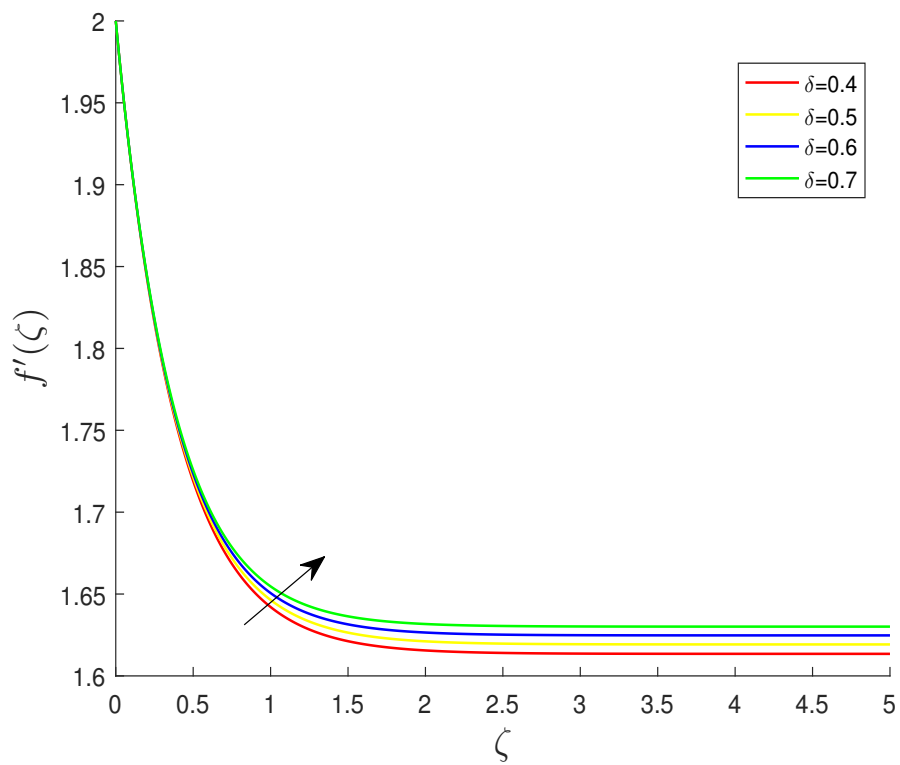


FIGURE 4.4: Impact of δ on the velocity profile.

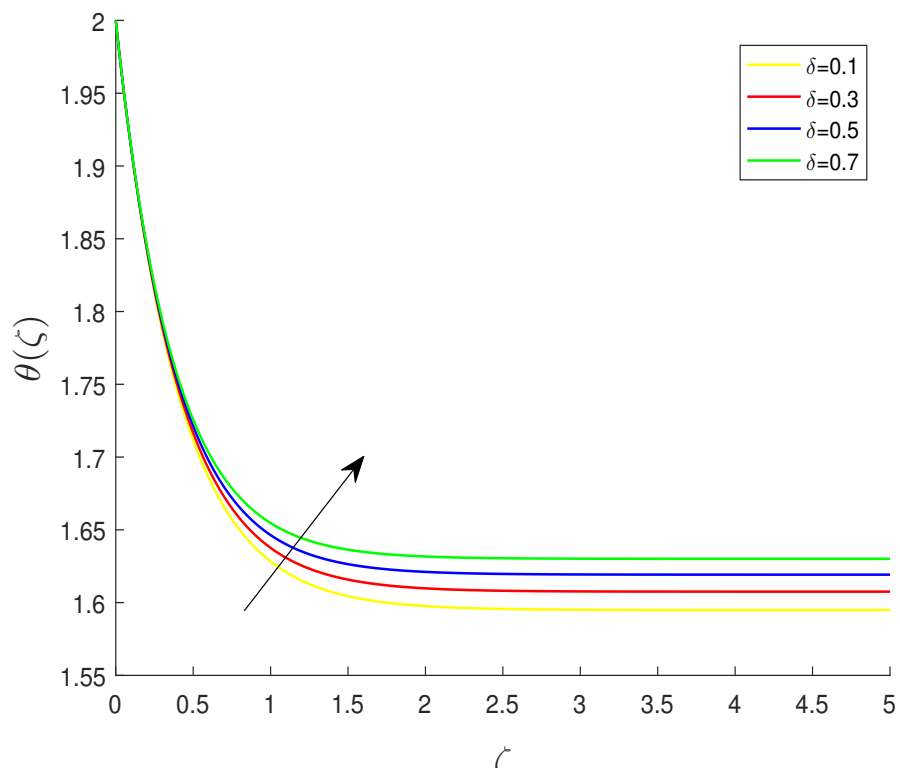


FIGURE 4.5: Impact of δ on the temperature profile.

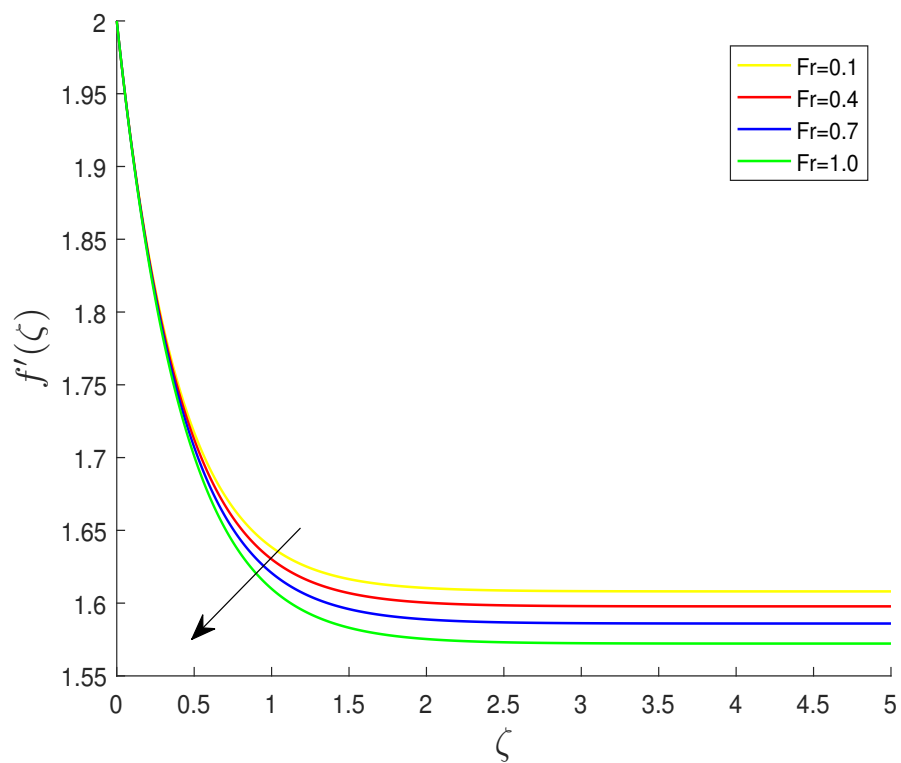


FIGURE 4.6: Impact of Fr on the velocity profile.

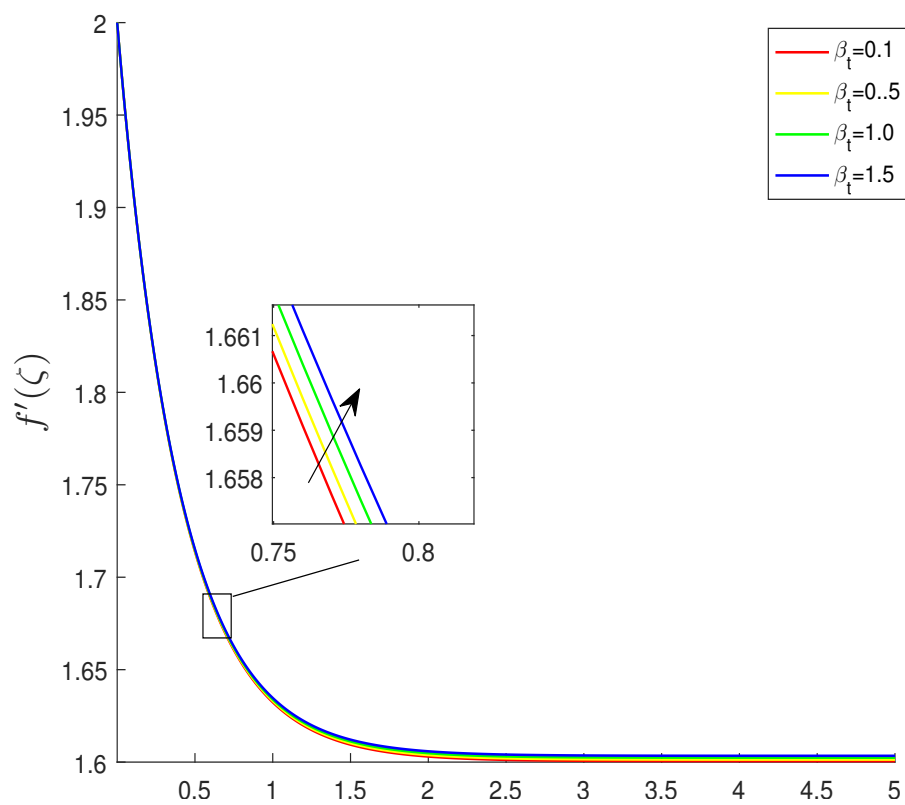


FIGURE 4.7: Impact of B_t on the velocity.

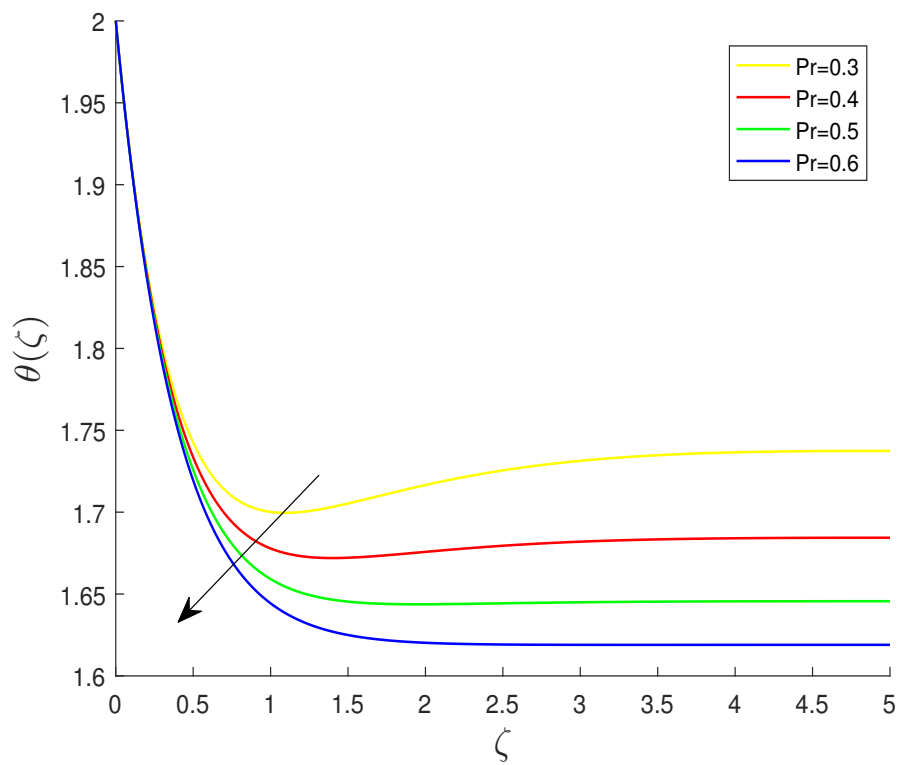


FIGURE 4.8: Impact of Pr on the temperature profile.

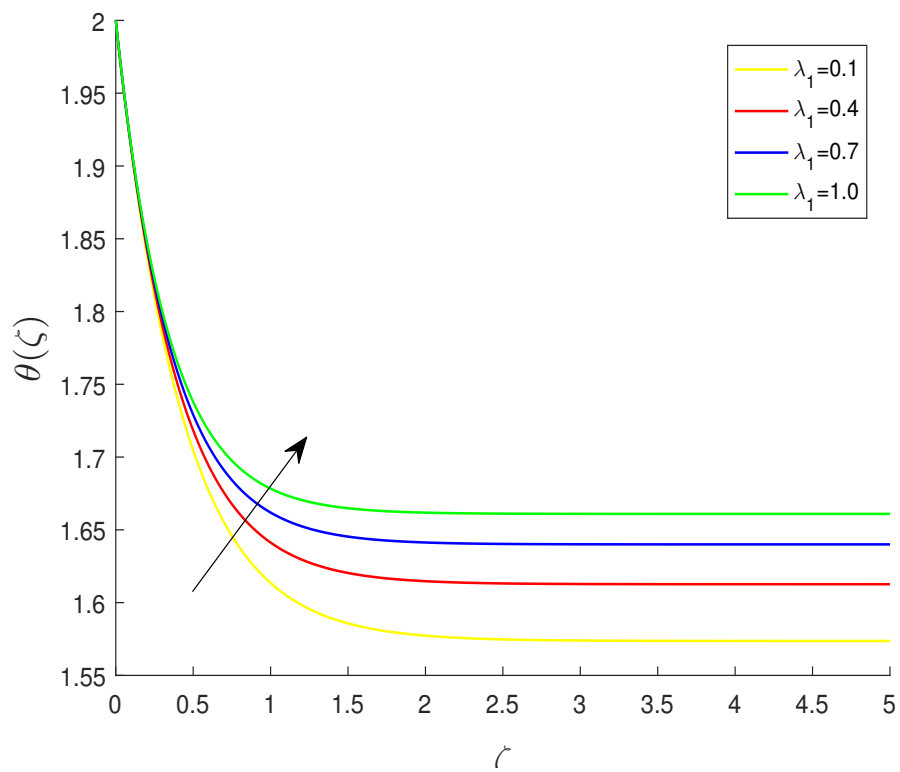


FIGURE 4.9: Impact of λ_1 on the temperature profile.

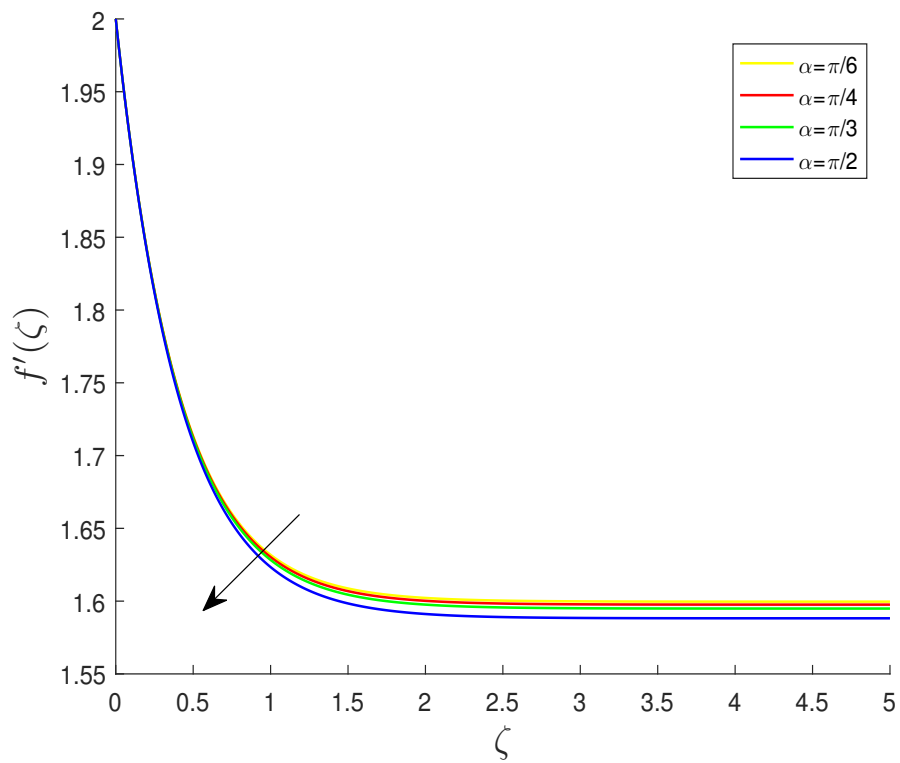


FIGURE 4.10: Impact of α on the velocity profile.

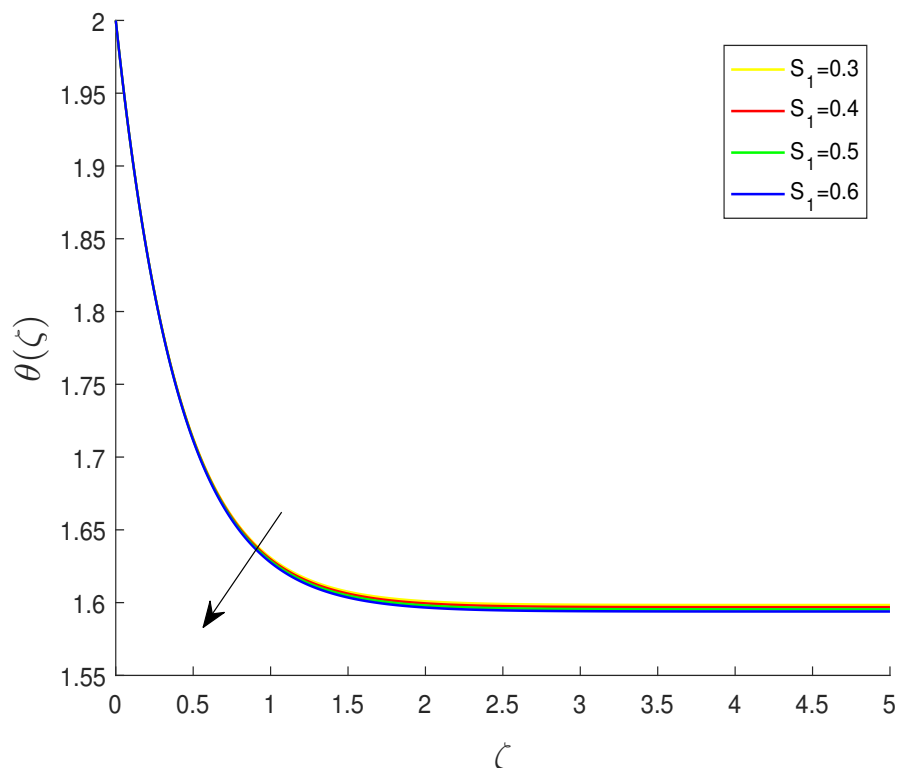


FIGURE 4.11: Impact of S_1 on the temperature profile.

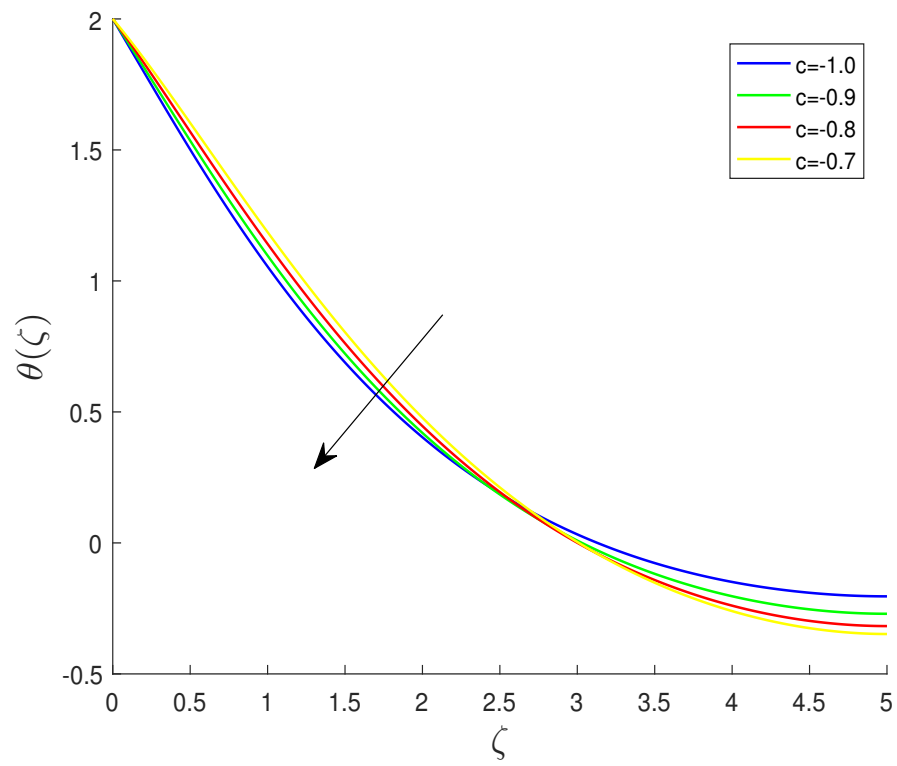


FIGURE 4.12: Impact of c on the temperature profile.

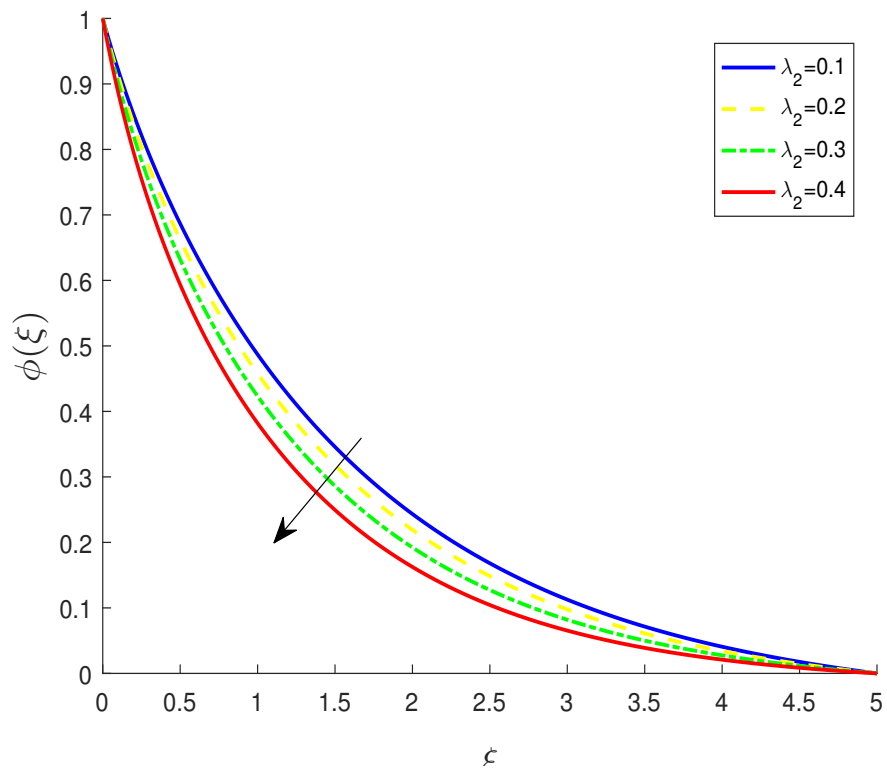


FIGURE 4.13: Impact of λ_2 on the concentration profile.

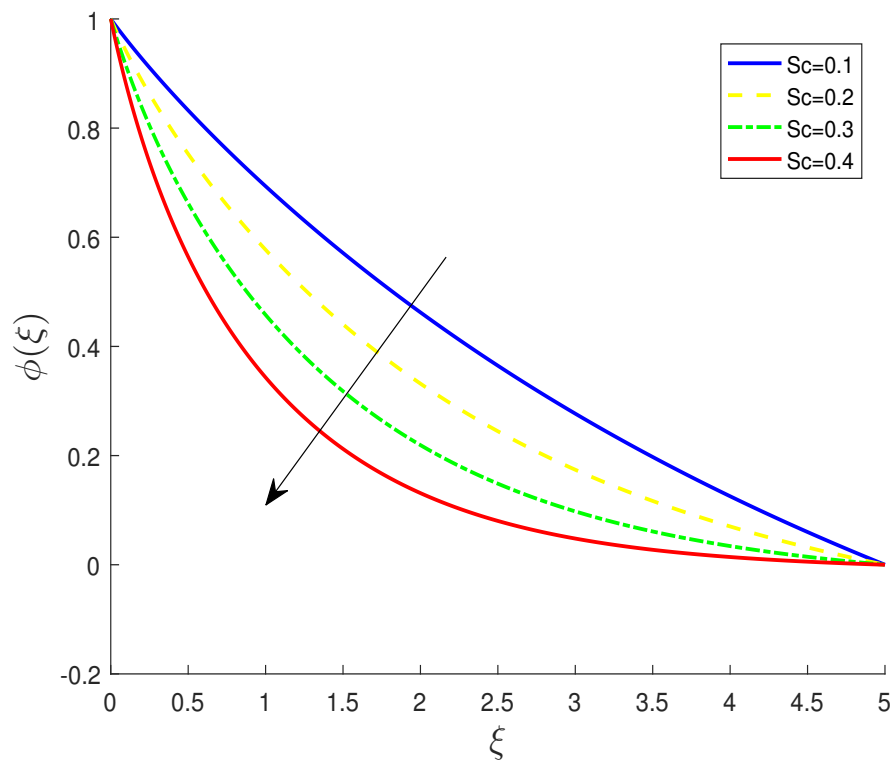


FIGURE 4.14: Impact of Sc on the concentration profile.

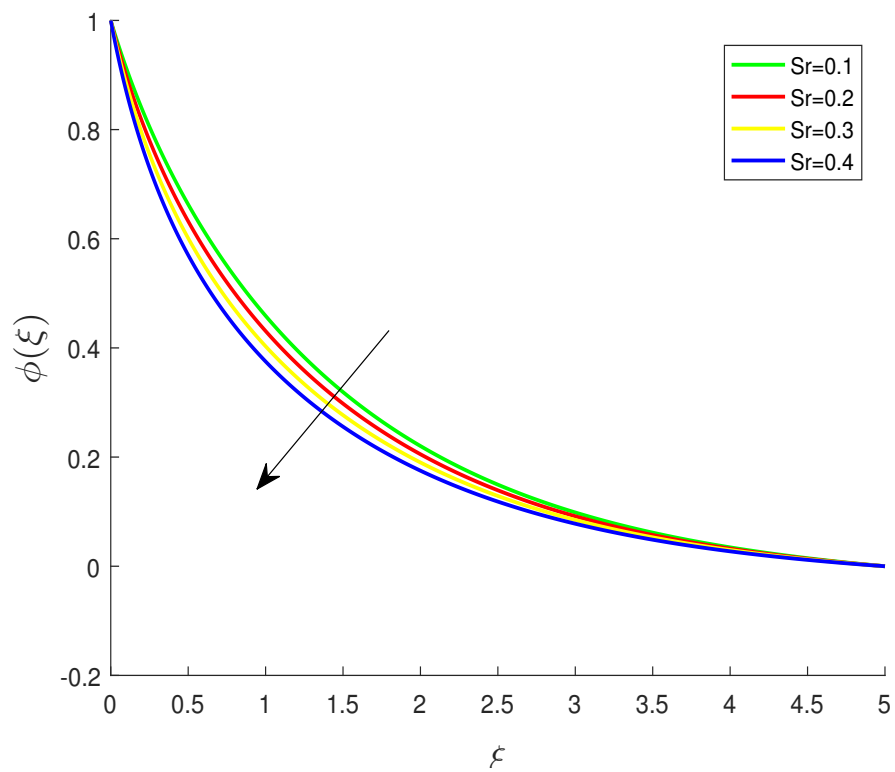
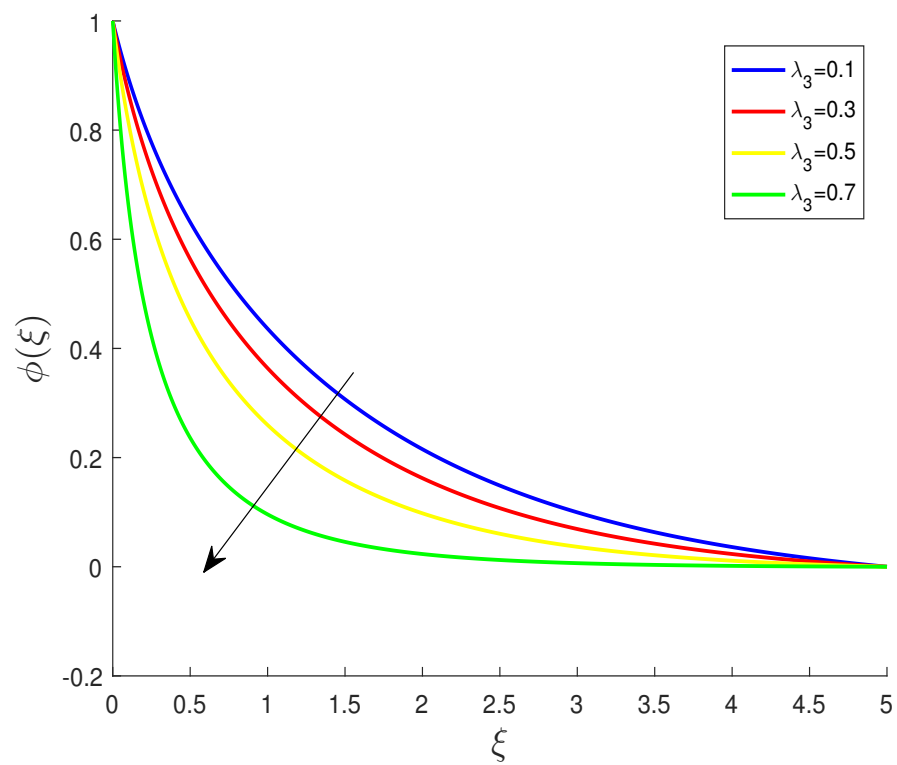


FIGURE 4.15: Impact of Sr on the concentration profile.

FIGURE 4.16: Impact of λ_3 on the concentration profiles.

Chapter 5

Conclusion

In this thesis, the work of Bilal et al. [33] is reviewed and extended by including the impact of Cattaneo-Christov, double diffusion and chemical reaction. First of all, momentum, temperature and concentration equations are converted into the ordinary differential equations by using similarity transformations. Numerical solution of ODEs has been obtained by using the shooting method. The results are represented through graphs and tables by using different parameters for velocity, temperature and concentration profiles. The achievements of the current research can be summarized as below:

- Increasing the values of the aligned angle γ , the velocity profile is decreased but the temperature and concentration profiles are increased.
- Due to rising the values of the Prandtl number Pr , the velocity and temperature profiles increase but concentration profile decrease .
- By rising the values of the magnetic parameter M causes an increase in the velocity, temperature and concentration profiles.
- An enhancement in the dimensionless Maxwell parameter β , the velocity, temperature and concentration profiles are increased.
- By boosting the values of the local inertia coefficient Fr , the velocity, temperature and concentration profiles are decreased

-
- The velocity, temperature and concentration profiles are increased due to an increment in the nonlinear thermal variable β_t .
 - Increasing the value of the porosity parameter λ_1 causes an increase in velocity and temperature profiles but a decrement in the concentration profile
 - By rising the values of the thermal stratification variable S_1 , the velocity, temperature and concentration profiles are decreased
 - Increasing the mixed convection variable δ causes an increment in the velocity, temperature and concentration profiles.
 - By increasing the shrinking parameter c , the velocity profile is increased but the temperature and concentration profiles are decreased.
 - Expanding the Schmidt number Sc , Soret number Sr and ϵ causes an increase in the concentration profile.

Bibliography

- [1] J. Thomason, P. Jenkins, and L. Yang, “Glass fibre strength—a review with relation to composite recycling,” *Fibers*, vol. 4, no. 2, p. 18, 2016.
- [2] B. C. Sakiadis, “Boundary-layer behavior on continuous solid surfaces: I. boundary-layer equations for two-dimensional and axisymmetric flow,” *AIChE Journal*, vol. 7, no. 1, pp. 26–28, 1961.
- [3] M. Turkyilmazoglu and I. Pop, “Heat and mass transfer of unsteady natural convection flow of some nanofluids past a vertical infinite flat plate with radiation effect,” *International Journal of Heat and Mass Transfer*, vol. 59, pp. 167–171, 2013.
- [4] J. Harris and W. Wilkinson, “Momentum, heat and mass transfer in non-newtonian turbulent flow in pipes,” *Chemical Engineering Science*, vol. 26, no. 3, pp. 313–320, 1971.
- [5] M. Ramzan, M. Bilal, J. D. Chung, and U. Farooq, “Mixed convective flow of maxwell nanofluid past a porous vertical stretched surface—an optimal solution,” *Results in Physics*, vol. 6, pp. 1072–1079, 2016.
- [6] M. Ramzan, M. Bilal, and J. D. Chung, “Influence of homogeneous-heterogeneous reactions on mhd 3d maxwell fluid flow with cattaneo-christov heat flux and convective boundary condition,” *Journal of Molecular Liquids*, vol. 230, pp. 415–422, 2017.
- [7] M. Bilal, M. Sagheer, and S. Hussain, “Three dimensional mhd upper-convected maxwell nanofluid flow with nonlinear radiative heat flux,” *Alexandria engineering journal*, vol. 57, no. 3, pp. 1917–1925, 2018.

-
- [8] L. J. Crane, "Flow past a stretching plate," *Zeitschrift für angewandte Mathematik und Physik ZAMP*, vol. 21, no. 4, pp. 645–647, 1970.
- [9] C.-R. Lin and C.-K. Chen, "Exact solution of heat transfer from a stretching surface with variable heat flux," *Heat and mass transfer*, vol. 33, no. 5, pp. 477–480, 1998.
- [10] M. Laha, P. Gupta, and A. Gupta, "Heat transfer characteristics of the flow of an incompressible viscous fluid over a stretching sheet," *Wärme-und Stoffübertragung*, vol. 24, no. 3, pp. 151–153, 1989.
- [11] M. Bilal, M. Sagheer, S. Hussain, and Y. Mehmood, "Mhd stagnation point flow of williamson fluid over a stretching cylinder with variable thermal conductivity and homogeneous/heterogeneous reaction," *Communications in Theoretical Physics*, vol. 67, no. 6, p. 688, 2017.
- [12] M. Ramzan, M. Bilal, S. Kanwal, and J. D. Chung, "Effects of variable thermal conductivity and non-linear thermal radiation past an eyring powell nanofluid flow with chemical reaction," *Communications in Theoretical Physics*, vol. 67, no. 6, p. 723, 2017.
- [13] M. Haroun, "On electrohydrodynamic flow of jeffrey fluid through a heating vibrating cylindrical tube with moving endoscope," *Archive of Applied Mechanics*, vol. 90, no. 6, pp. 1305–1315, 2020.
- [14] S. Akram, A. Razia, and F. Afzal, "Effects of velocity second slip model and induced magnetic field on peristaltic transport of non-newtonian fluid in the presence of double-diffusivity convection in nanofluids," *Archive of Applied Mechanics*, vol. 90, no. 7, pp. 1583–1603, 2020.
- [15] M. Turkyilmazoglu, "Effects of uniform radial electric field on the mhd heat and fluid flow due to a rotating disk," *International Journal of Engineering Science*, vol. 51, pp. 233–240, 2012.
- [16] M. Turkyilmazoglu, "Latitudinally deforming rotating sphere," *Applied Mathematical Modelling*, vol. 71, pp. 1–11, 2019.

- [17] M. Turkyilmazoglu, “Magnetic field and slip effects on the flow and heat transfer of stagnation point jeffrey fluid over deformable surfaces,” *Zeitschrift für Naturforschung A*, vol. 71, no. 6, pp. 549–556, 2016.
- [18] M. Turkyilmazoglu, “Mhd natural convection in saturated porous media with heat generation/absorption and thermal radiation: closed-form solutions,” *Archives of Mechanics*, vol. 71, no. 1, 2019.
- [19] I. Ullah, “Activation energy with exothermic/endothermic reaction and coriolis force effects on magnetized nanomaterials flow through darcy–forchheimer porous space with variable features,” *Waves in Random and Complex Media*, pp. 1–14, 2022.
- [20] M. Muskat, “The flow of homogeneous fluids through porous media,” *Soil Science*, vol. 46, no. 2, p. 169, 1938.
- [21] D. Pal and H. Mondal, “Hydromagnetic convective diffusion of species in darcy–forchheimer porous medium with non-uniform heat source/sink and variable viscosity,” *International Communications in Heat and Mass Transfer*, vol. 39, no. 7, pp. 913–917, 2012.
- [22] N. V. Ganesh, A. A. Hakeem, and B. Ganga, “Darcy–forchheimer flow of hydromagnetic nanofluid over a stretching/shrinking sheet in a thermally stratified porous medium with second order slip, viscous and ohmic dissipations effects,” *Ain Shams Engineering Journal*, vol. 9, no. 4, pp. 939–951, 2018.
- [23] B. Gireesha, B. Mahanthesh, P. Manjunatha, and R. Gorla, “Numerical solution for hydromagnetic boundary layer flow and heat transfer past a stretching surface embedded in non-darcy porous medium with fluid-particle suspension,” *Journal of the Nigerian Mathematical Society*, vol. 34, no. 3, pp. 267–285, 2015.
- [24] S. Rashidi, M. Dehghan, R. Ellahi, M. Riaz, and M. Jamal-Abad, “Study of stream wise transverse magnetic fluid flow with heat transfer around an obstacle embedded in a porous medium,” *Journal of Magnetism and Magnetic Materials*, vol. 378, pp. 128–137, 2015.

- [25] S. E. Ahmed, "Mixed convection in thermally anisotropic non-darcy porous medium in double lid-driven cavity using bejan's heatlines," *Alexandria Engineering Journal*, vol. 55, no. 1, pp. 299–309, 2016.
- [26] T. Hayat, F. Haider, T. Muhammad, and A. Alsaedi, "On darcy-forchheimer flow of viscoelastic nanofluids: A comparative study," *Journal of Molecular Liquids*, vol. 233, pp. 278–287, 2017.
- [27] Z. Kang, D. Zhao, and H. Rui, "Block-centered finite difference methods for general darcy–forchheimer problems," *Applied Mathematics and Computation*, vol. 307, pp. 124–140, 2017.
- [28] T. Sarpkaya, "Flow of non-newtonian fluids in a magnetic field," *AIChE Journal*, vol. 7, no. 2, pp. 324–328, 1961.
- [29] T. Hayat, M. Imtiaz, and A. Alsaedi, "Mhd 3d flow of nanofluid in presence of convective conditions," *Journal of Molecular Liquids*, vol. 212, pp. 203–208, 2015.
- [30] K.-L. Hsiao, "Mhd mixed convection for viscoelastic fluid past a porous wedge," *International Journal of Non-Linear Mechanics*, vol. 46, no. 1, pp. 1–8, 2011.
- [31] G. Ramesh, G. Manohar, P. Venkatesh, and B. Gireesha, "Significance of increasing lorentz force and buoyancy force on the dynamics of water conveying swcnt and mwcnt nanoparticles through a vertical microchannel," *Physica Scripta*, vol. 96, no. 8, p. 085209, 2021.
- [32] C. Raju, N. Sandeep, C. Sulochana, V. Sugunamma, and M. J. Babu, "Radiation, inclined magnetic field and cross-diffusion effects on flow over a stretching surface," *Journal of the Nigerian Mathematical Society*, vol. 34, no. 2, pp. 169–180, 2015.
- [33] M. Bilal and M. Nazeer, "Numerical analysis for the non-newtonian flow over stratified stretching/shrinking inclined sheet with the aligned magnetic

- field and nonlinear convection,” *Archive of Applied Mechanics*, vol. 91, no. 3, pp. 949–964, 2021.
- [34] R. W. Fox, A. McDonald, and P. Pitchard, *Introduction to Fluid Mechanics*. 2006.
- [35] R. Bansal, *A Textbook of Fluid Mechanics and Dydraulic Machines*. Laxmi publications, 2004.
- [36] J. Ahmed and M. S. Rahman, *Handbook of Food Process Design*. John Wiley & Sons, 2012.
- [37] J. N. Reddy and D. K. Gartling, *The Finite Element Method in Heat Transfer and Fluid Dynamics*. CRC press, 2010.
- [38] P. A. Davidson and A. Thess, *Magnetohydrodynamics*, vol. 418. Springer Science & Business Media, 2002.
- [39] M. Gad-el Hak, *Frontiers in Experimental Fluid Mechanics*, vol. 46. Springer Science & Business Media, 2013.
- [40] R. W. Lewis, P. Nithiarasu, and K. N. Seetharamu, *Fundamentals of the Finite Element Method for Heat and Fluid Flow*. John Wiley & Sons, 2004.
- [41] J. Kunes, *Dimensionless Physical Quantities in Science and Engineering*. Elsevier, 2012.